Development of a Laser-Pulse Compression Device based on Stimulated Brillouin Scattering

Master Thesis
by
Johan Norin

Lund Reports on Atomic Physics, LRAP-230
Lund, March 1998

This thesis was submitted to the
Faculty of Technology at Lund University
in partial fulfilment of the requirements for
the degree of Master of Science

Abstract

A laser pulse compressor based on stimulated Brillouin scattering has been developed and evaluated. It has been used to compress 7.5 ns pulses with a wavelength of 532 nm from one of the Nd:YAG lasers in the VUV laboratory at Lund high power laser facility. The compressed pulses have been led into a dye laser and after that into a KDP frequency doubling crystal. Pulse lengths of 950 ps directly after the SBS compressor, and of less than 300 ps after the KDP crystal have been measured.

Contents

1 Introduction

The Physics department of the Lund Institute of Technology has a laboratory for generation of laser pulses in the vacuum ultraviolet region of the spectrum (VUV-radiation). These pulses have a width of 5-7 ns and energy in the μJ region. The system needed to be upgraded to produce shorter pulses without lowering the power of the pulse.

The VUV pulses are obtained by mixing laser pulses from two "laser chains", both of which are working with pulses of 6-9 ns duration. To obtain shorter pulses in the VUV, one should reduce the pulse duration of at least one of the two laser chains.

To do this, a method based on Stimulated Brillouin Scattering (SBS) has been used. In principle, the pulse is led into a pipe with water. When half the pulse is in the pipe, the front of it is focused to initiate SBS and the pulse is reflected. A phenomenon called phase conjugation ensures that the pulse is reflected exactly the same way as it came. When the pulse travels back, the compression starts. The Brillouin scattering will turn the front of the returning wave into a mirror, which will gather the energy in the entire pulse into a short peak.

In this paper, the theory behind stimulated Brillouin scattering will be examined. The difficulties and advantages of the method will be discussed. The design of a practical compression unit will be described and the result from measurements with the compressor will be evaluated.

2 The Problem

To find a solution, we need a well-defined problem. In this chapter, we will examine the equipment present in the laboratory before the present upgrade. Some elementary laser physics needed to understand the problem will also be discussed.

2.1 Why do we want shorter pulses?

In spectroscopy, one examines the emission lines of different atoms and molecules, to find the proportions of the elements in the object we study. One tool of spectroscopy is lifetime measurements, or rather the determination of the transition probabilities. It is often quite easy to find the relations between the transition probabilities from a single level in an atom, although it is difficult to get absolute values. The lifetime of a level is the inverse of the sum of all the probabilities, and can thus be used to find the relative strengths (figure 2-1).

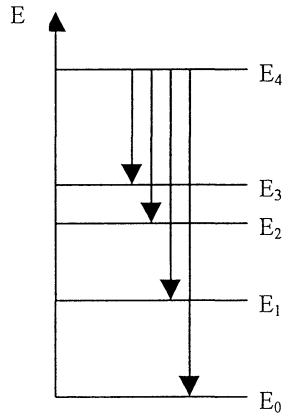

The transition probabilities A_{ij} determine the lifetime of the energy level.

$$A_{ij} = \left|\langle \varphi_i | e\vec{r} | \varphi_j \rangle\right|^2$$

To the left we have

$$\frac{1}{\tau_4} = \sum_{j=0}^{3} A_{4j}$$

Figure 2-1 Relations between transition probabilities and lifetimes.

There are many reasons for studying the lifetimes of energy levels. The resolution limit of any spectroscopic study is limited by the lifetime according to

$$\Delta\nu_{res} = \frac{1}{2\pi\tau} \tag{2.1}$$

In astrophysics, one uses the relative strength of different emission frequencies, to examine the relative abundance of the elements in e.g. stars and nebulae. For this to be done, the relative strengths of the spectral lines must be known. Until recently there has been no possibility to perform astronomical observations in

the far ultraviolet region, since air (or rather oxygen, carbon dioxide and water vapours) absorbs strongly and is thus opaque at wavelengths below 200 nm. The launching of various orbital telescopes and spectrometers (especially the Hubble Space Telescope in 1990) has opened this window [1].

These VUV frequencies mainly originate from transitions in ions, as the electron cloud of an ion is more tightly bound to the nucleus than that of a neutral atom. Cosmic ion concentrations are of course of interest in astro-physics, but since the oscillator strengths of ions have been of only limited interest before, few laboratory studies are available for comparison. A new need of laboratory measurements has suddenly arisen.

If the lifetime of a certain level in an atom is to be measured, we populate the level with a short pulse of corresponding energy and study the emission when it returns to lower energy levels. The time evaluation of this emission will be a convolution of the decay after an infinitely short pulse and the exciting pulse (figure 2-2). To calculate the true pulse shape of the spontaneous decay, one needs to de-convolute the observed emission. This can be done with small errors only if the fall time of the exciting pulse is shorter (or at least not much longer) than the lifetime studied. To measure the lifetimes of excited states when shorter than a few nano-seconds, the standard setup in the VUV laser laboratory is inadequate. The generated pulses' duration of 6-9ns must be reduced.

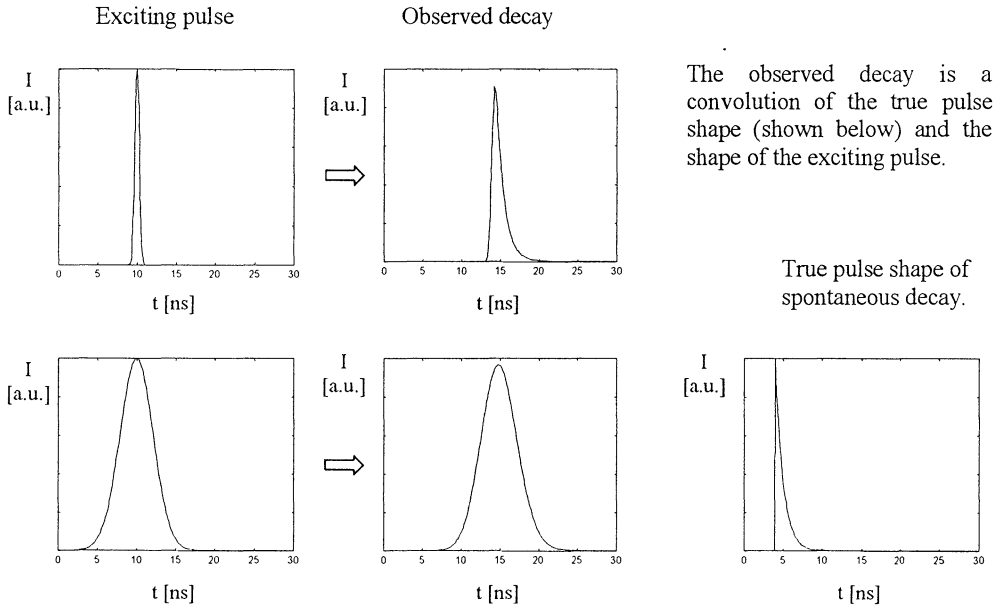

Figure 2-2 Observed decay after excitation, compared with the true decay-curve. In the top raw, the duration of the exciting pulse is shorter than the lifetime of the excited state. In the lower raw, it is longer.

2.2 Spectral Shape of a Pulse

A pulse can be fully characterised in either the time or the frequency plane. These are tightly connected, and are mathematically each others Fourier transforms.

2.2.1 Bandwidth-Lifetime

Since the accuracy of a lifetime measurement depends of the pulse length, there seems to be no apparent reason not to make the pulses as short as possible. However, if a pulse is made shorter, the bandwidth of it will be larger, due to ordinary Fourier transformation. Suppose we have an ideal Gaussian pulse with a maximum intensity I_{max} and a pulsewidth of τ (FWHM)

$$I(t) = I_{max} e^{-4\ln(2)\frac{t^2}{\tau^2}} \tag{2.2}$$

The field will oscillate as

$$E(t) = E_{max} e^{-2\ln(2)\frac{t^2}{\tau^2}} \left(\frac{1}{2} e^{-i\omega_0 t} + c.c. \right) \tag{2.3}$$

In the frequency plane, the pulse will be

$$E(\omega) = k \left[e^{-\frac{\tau^2(\omega+\omega_0)^2}{8\ln 2}} + e^{-\frac{\tau^2(\omega-\omega_0)^2}{8\ln 2}} \right] \tag{2.4}$$

For the positive peak, the intensity is

$$I(\omega) = I_{max} e^{-\frac{\tau^2(\omega-\omega_0)^2}{4\ln 2}} \tag{2.5}$$

then, the bandwidth of the pulse is

$$\Delta\omega = \frac{4\ln(2)}{\tau} \tag{2.6}$$

From this, we can see that

$$\Delta\omega \cdot \tau = 4\ln(2) \tag{2.7}$$

As we can see, an 8 ns pulse has a minimum bandwidth of 56 MHz. If we use a shorter pulse with a duration of 80ps, the minimum bandwidth is 5.6 GHz. The problem arises when we want to examine a certain energy level. The bandwidth of the pulse must then be sharp enough in order to efficiently excite the level of interest, and the duration short enough to resolve the spontaneous decay. This is indeed an act of balance.

2.2.2 Longitudinal Laser Modes

The frequency of a laser is determined mainly by two things. The width of the transition used to obtain the laser radiation, and the geometry of the cavity. A cavity can radiate on all frequencies allowing a standing wave with the nodes on the end mirrors to be formed. The spacing between two such frequencies is

$$\Delta\nu_{mode} = \frac{c}{2nL} \tag{2.8}$$

there nL is the optical length of the cavity and c the speed of light in vacuum. If a lasing medium is placed in the cavity, certain modes will be amplified, leading to the mode-structure of figure 2-3. In the figure, numerical values for the Nd:YAG laser has been used [2].

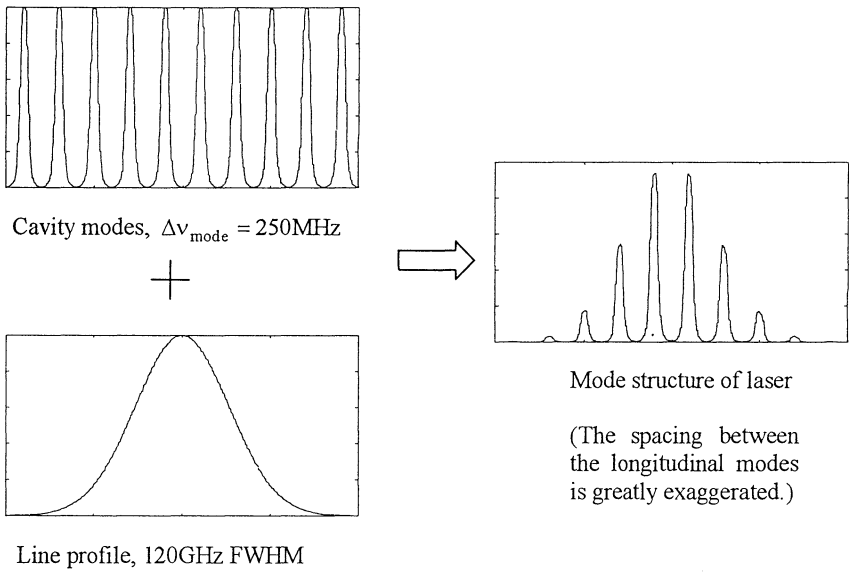

Figure 2-3 Mode structure of the Nd:YAG laser. A lot of cavity modes will fit in the line profile of the active lasing medium.

If the laser radiation contains several frequency components, the temporal shape will differ from that of a single mode. In figure 2-4, twelve similar pulses of different frequencies are added. If the phase of the different component can be kept under control, very short pulses can be created, but if the phase varies randomly, the temporal profile will be distorted.

2.3 Equipment

In the VUV (Vacuum Ultra Violet) laboratory a system of lasers are used to generate vacuum ultraviolet laser radiation. Two Nd:YAG lasers are used to produce light at 532 nm. The radiation from one of them feeds a dye laser,

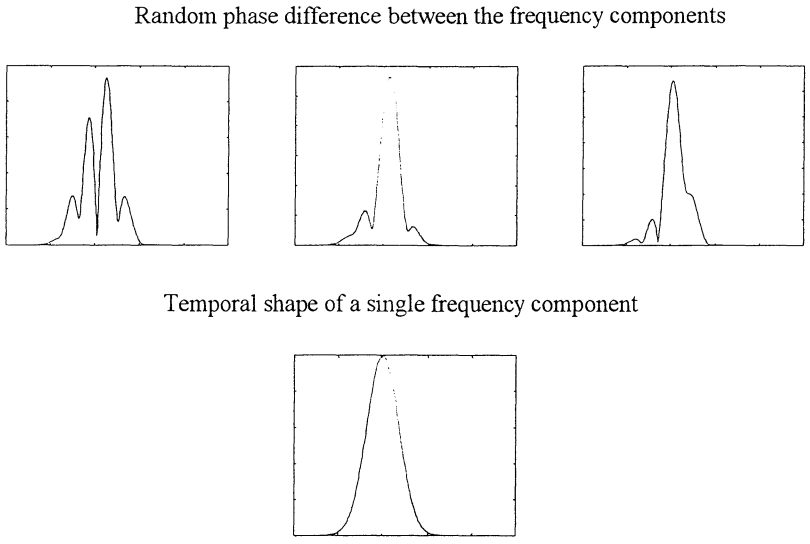

Figure 2-4 If a pulse contains several frequency-components of random phase, the temporal shape of the pulse will be distorted.

which is used to generate red light at 637.65 nm. This red light is first put into a frequency doubling crystal, and thereafter mixed with the original light. The effect is ultraviolet radiation at 212.55 nm. The other Nd:YAG laser feeds either a tuneable Ti:Sapphire laser or another dye laser. The output is mixed with the 212 nm-radiation in a Kr-gas cell, to produce the tuneable VUV radiation. Below the different parts of the process will be examined closer.

2.3.1 The Nd:YAG Laser

The abbreviation Nd:YAG means Neodym:Yttrium-Aluminium-Garnet, and describes a solid state four level laser. The energy levels are shown in figure 2-5. The laser is pumped by flash lamps to excite the Nd^{3+}-ions imbedded in the $YalO_3$-crystal. Several high energy levels are then populated, but the ions soon "falls" to a quasi-stable level of lower energy ($^4F_{3/2}$). The Q-value of the laser (the "laser-efficiency") is kept low to prevent lasing, until a large enough population is built up in this level. Then the Q-value is switched, the laser starts to radiate and the population falls to level $^4I_{11/2}$, which is rapidly depopulated as the ions return to the ground state. As a result, the laser emits a high-energy pulse in a very short time. The original pulse is at 1064 nm, and this light is frequency doubled in a nonlinear crystal to produce the output of 532 nm [2]. The laser used is a Continuum NY82-10 injection-seeded Nd:YAG-laser (see figure 2-6 for layout). Its main parts are the seeder, the active Q-switch, the oscillator, the preamplifier, the main amplifier, and the doubling crystal.

The seeder is a monolithic, laser diode pumped, unidirectional ring resonator. Since it is a ring laser, the resonator is a travelling instead of a standing wave. As such it does not suffer from spatial hole burning, and will lase with a single frequency. When the radiation from the seeder is led into the oscillator, it initiates oscillation on that frequency.

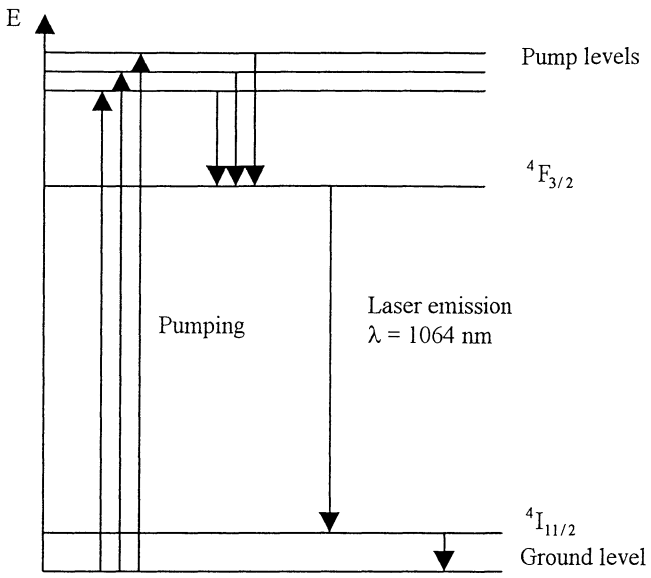

Figure 2-5 Energy levels in a Nd:YAG laser.

The Q-switch consists of a quarter wave plate, a pockels cell and a polarizer. Its function is to block one of the mirrors of the oscillator cavity. Shortly after the Nd:YAG rod has been excited by the flash lamps, the Q-switch opens and laser radiation can build up in the cavity. In case of no seeding, the laser radiation will build up from spontaneous noise. If seed emission on a frequency near a longitudinal mode of the oscillator is led into the cavity, it will dominate over the noise, and that mode will contain more than 1000 times the energy of any other mode.

After the oscillator, the pulse is led into the preamplifier and the main amplifier. After that, it will have duration of 7-10 ns and energy of up to 1400 mJ at 1064nm. Since we are interested in 532 nm radiation, we insert a doubling crystal into the beam. (The function of the crystal will be discussed below). After that, we have a 750 mJ pulse of 6-9 ns duration [3].

2.3.2 The Dye Laser

A dye laser uses a broadband dye as active medium. To get a certain frequency as output, a suitable dye is selected. The fine adjustment is achieved by turning a grating in the oscillator cavity.

The laser being used is a Continuum ND60 dye laser. The pump beam is divided into three beams, which pump the oscillator, the pre-amplifier and the main amplifier. In VUV-generation, the dye DCM with a peak wavelength of 635.5 nm is used solved in methanol. The grating is turned by a computer to produce radiation at 638 nm.

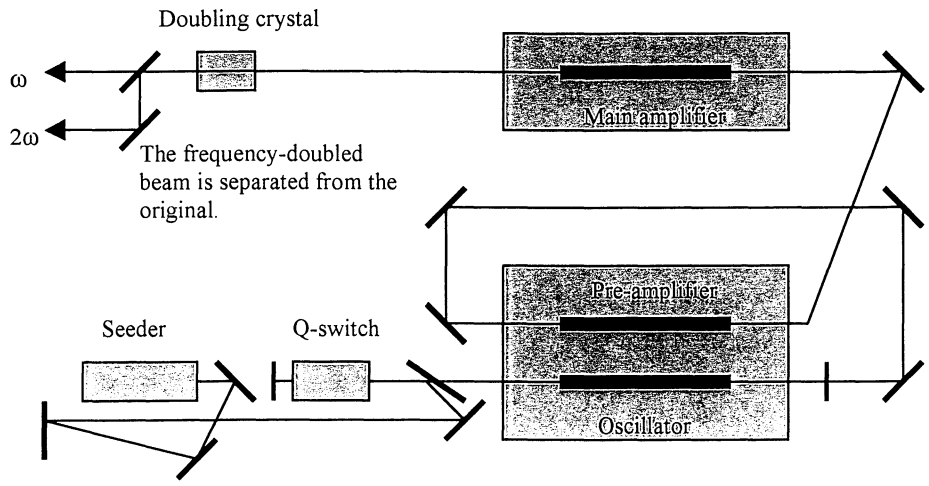

Figure 2-6 Layout of the Nd:YAG Laser.

2.3.3 The Doubling Crystal

A doubling crystal is made of a nonlinear optic material. The polarization of the crystal exposed to an intense field becomes:

$$\tilde{P} = \varepsilon_0\left(\chi^{(1)}E + \chi^{(2)}E^2 + \chi^{(3)}E^3 + \ldots\right) \tag{2.9}$$

In a homogenous crystal the even terms vanishes due to symmetry [4].

In the Nd:YAG laser a KD*P-crystal (KD_2PO_4) is used, and after the dye laser a KDP-crystal (KH_2PO_4). Apart from doubling the frequency of the light, the pulsewidth is shortened. A pulse with a Gaussian time-profile of

$$I = I_{max}e^{-4\ln(2)\frac{t^2}{\tau^2}} \tag{2.10}$$

will have a field amplitude of

$$E = E_{max}e^{-2\ln(2)\frac{t^2}{\tau^2}} \tag{2.11}$$

After the doubling crystal, the field amplitude would have the temporal form of

$$E_{doubled} = k_1 E_{max}^2 e^{-4\ln(2)\frac{t^2}{\tau^2}} \tag{2.12}$$

and the intensity of the frequency-doubled light would then be

$$I_{doubled} = k_2 I_{max}^2 e^{-8\ln(2)\frac{t^2}{\tau^2}} \tag{2.13}$$

As we can see, the pulsewidth is now a factor $\sqrt{2}$ shorter (see figure 2-7).

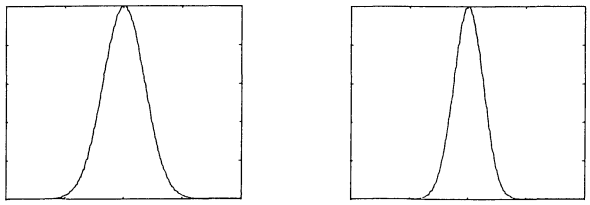

Figure 2-7 Compression as an effect of frequency doubling.

Unfortunately the described process only works for very weak signals. In our case the crystal is saturated and therefore the pulse shortening will not be that efficient. However, the duration will still be shortened by between 10 and 15 percent.

2.3.4 VUV Radiation

The radiation from the second Nd:YAG laser is used to pump a broadband tuneable Ti:Sapphire laser, or a second dye laser. As output, we have radiation of variable wavelength. The beam from this laser is mixed with the 212 nm beams in a cell with krypton gas, resulting in VUV-radiation. As we can see in the energy-level-diagram of figure 2-8, we can by changing the wavelength of the second laser tune the VUV-radiation to an arbitrary wavelength. The 212 nm radiation is tuned to be two-photon resonant with the upper energy level, which is populated by two-photon absorption. The second laser will depopulate the level into a virtual level, from where the atom relaxes to the ground state, emitting VUV radiation. The process is called "resonant 4-wave sum difference mixing".

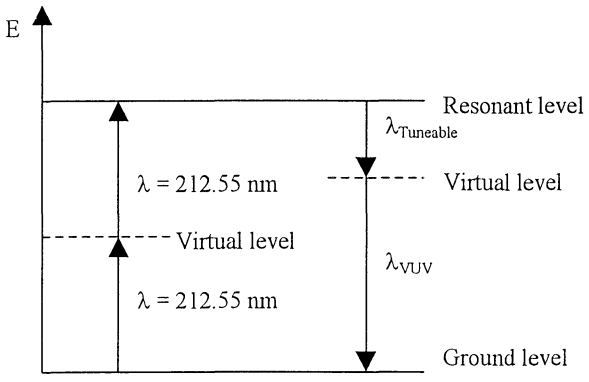

Figure 2-8 Energy levels of VUV-generation

3 Solutions to the Problem

The problem, as we have seen, is that the present pulse is too long to resolve the lifetimes we want to measure. In the room next to the VUV-laboratory, there is a system generating picosecond pulses. The shortness of these pulses is sufficient, but their mathematically unavoidable broad bandwidth, makes them less suitable. The best pulse width should be of about 1 ns, but unfortunately, laser systems producing pulses of this length are rare.

We have two options. Either to cut the existing pulse by some means, or to compress it.

3.1 Compression of Fourier-Limited Pulses

As we have seen before, there is a close connection between the bandwidth and the duration of the pulse. This can cause problems when we want to compress the pulses, since it gives us a theoretical lower limit of the pulse duration. The Nd:YAG laser has a bandwidth of 850 MHz [3], which, according to eq. (2.7), gives a minimum duration of 3.3 ns. If the compression shall work, we need to create new frequency components.

3.2 Active Cutting of Pulses

An easy way to get around the bandwidth problem is to simply cut the pulse. The cutting will always take some short period of time, and the transient itself will contain the frequencies necessary.

The actual cutting can be done with a pockels cell and some triggering device, but the redundant energy will be absorbed, which is a "waste" of photons. The triggering may cause problems, since we need some kind of delay before the pockels cell. The Nd:YAG laser has a jitter of approximately 1 ns, which would cause the energy of the cut pulse to fluctuate if the cell would be trigged by the electronics of the laser. Instead, one could build a delay line, but then the spatial profile of the beam would be distorted.

3.3 Passive Methods

A big advantage of compression methods are that they are passive; there are no need for triggering. The problem of limited bandwidth can be solved if we find a compression method which can create new frequency components. As we shall see in the next chapter, Stimulated Brillouin Scattering offers a simple solution to the problem.

4 Stimulated Brillouin Scattering

When a beam of light is scattered by an acoustic wave, we have Brillouin scattering. When the acoustic wave itself is formed by the same (very intense) light, we have Stimulated Brillouin Scattering (SBS). It has been shown that stimulated Brillouin scattering can be useful for pulse compression in our energy region [5-7]. The basic principles of the process are easy. The original beam is focused into some kind of medium. The spontaneously scattered light will then interfere with the original beam, and a pattern of standing waves is formed. If the intensity is high enough, the pressure in the medium will change due to electrostriction. The pressure causes density changes corresponding to the standing light waves in the medium. As the density varies, so does the refractive index, and an interference mirror is formed. If the light is reflected from this mirror in the opposite direction of the original beam, the pressure waves (acoustic waves) and the scattered light will amplify each other.

Once the mirror is formed, it moves with the front of the back-scattered light. At first sight, one might find it strange with acoustic waves travelling with the speed of light, but it must be kept in mind that it is only the envelope of the wave that is moving. The actual waves are moving in the opposite direction with a considerably lower speed. In fact, they hardly move at all during the short period of time it takes for the optical pulses (first the original and then the scattered) to pass.

4.1 A Brief History

Although Brillouin scattering has been known for a long time, the first article concerning SBS was published in 1964 [8]. The authors, R. Y. Chiao, C. H. Townes and B. P. Stoicheff detected SBS in quartz and sapphire from a maser beam. They noted that the scattered radiation was very intense. In fact, the intensity of the scattered wave was of the same order of magnitude as in the incident beam, and the crystals often ruptured due to the high local stresses produced by the acoustic waves.

The first time the possibility of SBS as a pulse compressor method was published, was when one noted strange damages in optical fibres [5]. Since then the research on the topic has accelerated, and SBS compressors dealing with pulse energies of up to 25 J have been developed [9].

There are many articles published on the subject by researchers from the former Soviet Union. When looking for them, it is a great help to know that Brillouin scattering in Russian papers is named Mandel'shtam scattering.

4.2 Theory

The SBS process can be described by a system of three nonlinear differential equations. Two of which determines the behaviour of the original and the scattered light fields, and one that describes the acoustic wave. Unfortunately, this system does not have an analytic solution for an arbitrary pulse, but it is

possible to find some interesting properties of the process. We will derive the largest allowed bandwidth for the incident beam. Thereafter we will examine the acoustic waves, and discuss how the phonon lifetime limits the compression ratio. Finally, we will look at the threshold value, i.e. the minimum intensity of original light needed for the process to start, and compare this with measurements.

In order to do this, we must first have expressions for the three waves and we must know how they couple to each other. The presentation follows the same steps as in ref. [4], but with the SI-system instead of the Gaussian. The emphasis will be on the parts that tells us how to construct the SBS compressor, or that can be directly compared with measurements.

4.3 Magnitude of the Stokes Shift

The original and the stoke shifted fields can be written

$$\tilde{E}_1(z,t) = \tfrac{1}{2} E_1(z,t) e^{i(k_1 z - \omega_1 t)} + \text{c.c.} \tag{4.1a}$$

$$\tilde{E}_2(z,t) = \tfrac{1}{2} E_2(z,t) e^{i(k_2 z - \omega_2 t)} + \text{c.c.} \tag{4.1b}$$

The tildes are used to describe a rapidly oscillating variable, while the same variable without the tilde are used when we treats the more slowly changing amplitude.

The acoustic (density) wave can be written in a similar way

$$\tilde{\rho}(z,t) = \tfrac{1}{2} \rho(z,t) e^{i(qz - \Omega t)} + \text{c.c.} \tag{4.2}$$

with $\tilde{\rho}(z,t)$ as the deviation from the mean density.

To find the relations between the frequencies and the wave vectors, we use the laws of conservation of energy and momentum. In the SBS process, an incoming photon with energy $\hbar\omega_1$ and momentum $\hbar k_1$ is scattered. After the scattering, we have a photon moving in the opposite direction (energy $\hbar\omega_2$ and momentum $k\omega_2$), and an acoustic phonon (energy $\hbar\Omega$ and momentum $\hbar q$), moving in the same direction as the original photon (figure 4-1). We will see later why the scattering occurs for these directions only.

The conservation of energy gives us

$$\hbar\omega_1 = \hbar\omega_2 + \hbar\Omega \tag{4.3}$$

while the conservation of momentum yields

$$\hbar q = \hbar k_1 + \hbar k_2 \tag{4.4}$$

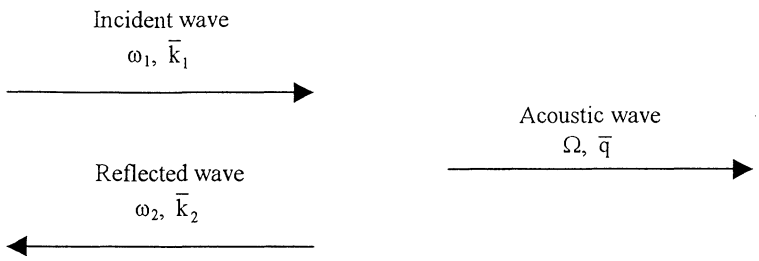

Figure 4-1 Elastic photon-phonon scattering.

Momentum is formally a vector, but since all movements are in one dimension, we write it as a scalar instead. When doing this it is important to keep track of the signs of the different k's. Note that $k_1 \approx k_2$ but $\bar{k}_1 \approx -\bar{k}_2$.

Since $k_i = \frac{n\omega_i}{c}$ and $q = \frac{\Omega}{v}$ we can rewrite the last equation as

$$\Omega = \frac{nv}{c}(\omega_1 + \omega_2) \tag{4.5}$$

where v is the speed of sound and n is the refractive index of the media.

By combining eq. (4.3) and eq. (4.5) we form

$$\Omega = \frac{2nv}{c + nv}\omega_1 \tag{4.6}$$

and

$$q = \frac{2k_1}{1 + \frac{nv}{c}} \tag{4.7}$$

Since $v << \frac{c}{n}$ we can approximate these equations to

$$\Omega \approx \frac{2nv}{c}\omega_1 \tag{4.8}$$

$$q \approx 2k_1 \tag{4.9}$$

The velocity of sound is well known for most liquids and gases, so we can now (if the frequency of the original light is known) describe the interacting waves. Typical values of the stoke shift Ω are between 4 and 11 GHz for liquids. Since the shift is proportional to the velocity of sound in the medium, it is higher in most solids and lower in most gases.

For water at room temperature and with an original beam of wavelength 532 nm, the shift is 7440 MHz ($\approx$ 0.007nm).

4.3.1 Electrostriction

The whole phenomena of stimulated Brillouin scattering depends on the fact that electric fields induce pressure in dielectrics. We will see later that the origin on the acoustic wave is this pressure, and we must thus know how it depends on the applied field. The electrostatic energy density in a material subjected to an electric field can be found in most textbooks treating electromagnetics [11,12]. We have

$$u_E = \frac{1}{2}\varepsilon E^2 \tag{4.10}$$

where ε is the dielectric permittivity of the medium. The unit of u_E is energy per unit volume, which might be confusing since we can not localize the energy within the field. The reason that the term is used is that it gives the correct value of the total energy, when it is integrated over the volume. For small differences in the permittivity we have

$$\Delta u_E = \frac{1}{2}\Delta\varepsilon E^2 \tag{4.11}$$

The change in permittivity can be expressed

$$\Delta\varepsilon = \left.\frac{\partial\varepsilon}{\partial\rho}\right|_T \Delta\rho + \left.\frac{\partial\varepsilon}{\partial T}\right|_\rho \Delta T \approx \frac{\partial\varepsilon}{\partial\rho}\Delta\rho \tag{4.12}$$

The last approximation can be made since the permittivity is only weakly dependent on the temperature of the material.

If we assume that no heat enters or leaves the volume, a decrease in energy must equal the work done by the volume upon its surroundings and vice versa. The volume will then change according to

$$\Delta u_E = \Delta w = \frac{p\Delta V}{V} = -p\frac{\Delta\rho}{\rho} \tag{4.13}$$

By combining (4.12) and (4.13) we can see that the pressure in the material depends on the applied field according to

$$p = -\frac{1}{2}\frac{\partial\varepsilon}{\partial\rho}\rho E^2 \tag{4.14}$$

Now we introduce the electrostrictive constant. It describes how the pressure in a material is changed by the electric field. In the literature, the constant is defined most often as

$$\gamma_e \equiv \rho\frac{\partial\varepsilon}{\partial\rho} \tag{4.15}$$

meaning that we can write the change in pressure as

$$p = -\frac{1}{2}\gamma_e E^2 \tag{4.16}$$

4.3.2 The Wave Equations

We start with Maxwell's familiar equations

$$\nabla \times \overline{E} = -\frac{\partial \overline{B}}{\partial t} \tag{4.17a}$$

$$\nabla \times \overline{H} = \overline{J} + \frac{\partial \overline{D}}{\partial t} \tag{4.17b}$$

$$\nabla \cdot \overline{D} = \rho \tag{4.17c}$$

$$\nabla \cdot \overline{B} = 0 \tag{4.17d}$$

We also assume that there are no currents present, $\overline{J} = 0$, and that the material is non-magnetic, with $\overline{B} = \mu\overline{H}$. It can, however, be polarized with

$$\overline{D} = \varepsilon_0\overline{E} + \overline{P} = \varepsilon_0\overline{E} + \varepsilon_0(\chi\overline{E} + \chi^{(2)}E^2 + \chi^{(3)}E^3 + \ldots) = \varepsilon\overline{E} + \overline{P}_{NL} \tag{4.18}$$

A rather straightforward calculation then gives the wave equation.

We start by taking the rotation of eq. (4.17a) and then change order of derivation.

$$\nabla \times \nabla \times \overline{E} = \nabla \times \left(-\frac{\partial \overline{B}}{\partial t}\right) = -\frac{\partial}{\partial t}\left(\nabla \times \overline{B}\right) \tag{4.19}$$

After that we replace $\overline{B}$ with $\mu_0\overline{H}$ and insert eq. (4.17b)

$$-\frac{\partial}{\partial t}\left(\nabla \times \overline{B}\right) = -\mu\frac{\partial}{\partial t}\left(\nabla \times \overline{H}\right) = -\mu\frac{\partial^2}{\partial t^2}\overline{D} = -\mu\frac{\partial^2}{\partial t^2}\left(\varepsilon\overline{E} + \overline{P}_{NL}\right) \tag{4.20}$$

If we use the vector identity

$$\nabla \times \nabla \times \overline{E} = \nabla \cdot \left(\nabla \cdot \overline{E}\right) - \nabla^2\overline{E} \tag{4.21}$$

we obtain the equation

$$\nabla \cdot \left(\nabla \cdot \overline{E}\right) - \nabla^2\overline{E} = -\mu\frac{\partial^2}{\partial t^2}\left(\varepsilon\overline{E} + \overline{P}_{NL}\right) \tag{4.22}$$

Now we make our first approximation. Since we are primarily interested in highly parallel laser radiation, we assume $\overline{E}$ to be an infinite plane wave. The divergence of the field is then zero, and the leftmost term of eq. (4.22) vanishes identically. We also write eq. (4.22) in one dimension. If we collect all terms with the $\overline{E}$-field on one side, we have the final equation:

$$\frac{\partial^2}{\partial z^2}E(z,t)-\mu\varepsilon\frac{\partial^2}{\partial t^2}E(z,t)=\mu\frac{\partial^2}{\partial t^2}P_{NL}(z,t) \tag{4.23}$$

Note that the polarization acts as a driving term for the wave equation, and that all kinds of polarization in the materiel must be accounted for. The question is how the polarization is affected by the fields in the material. We have

$$\overline{P}_{NL}=\Delta\varepsilon\overline{E} \tag{4.24}$$

By using eq. (4.12) we can write

$$\Delta\varepsilon=\frac{\partial\varepsilon}{\partial\rho}\Delta\rho=\gamma_e\frac{\Delta\rho}{\rho_0} \tag{4.25}$$

From now on ρ_0 will be used for the mean density of the medium.

The nonlinear polarization, which acts as the driving term of the wave equation, can be written

$$P_{NL}=\frac{\gamma_e}{\rho_0}\left(\tilde{\rho}\tilde{E}\right) \tag{4.26}$$

This polarization has many terms with different frequencies and wave vectors, and to determine which parts of it that affects a certain field, the components must be studied.

$$\tilde{\rho}\tilde{E}=\tfrac{1}{4}\left[\rho e^{i(qz-\Omega t)}+c.c.\right]\left[E_1e^{i(k_1z-\omega_1t)}+E_2e^{i(-k_2z-\omega_2t)}+c.c.\right]=$$

$$=\tfrac{1}{4}\left[\rho E_1e^{i((q+k_1)z-(\Omega+\omega_1)t)}+\rho^*E_1e^{i((-q+k_1)z-(-\Omega+\omega_1)t)}+\rho E_2e^{i((q-k_2)z-(\Omega+\omega_2))}+\right.$$

$$\left.+\rho^*E_2e^{i((-q-k_2)z-(-\Omega+\omega_2))}\right]+c.c.=$$

$$=\tfrac{1}{4}\left[\rho E_1e^{i((q+k_1)z-(\Omega+\omega_1)t)}+\rho^*E_1e^{i(-k_2z-\omega_2t)}+\rho E_2e^{i(k_1z-\omega_1t)}+\rho^*E_2e^{i(-(q+k_2)z-(\omega_2-\Omega)t)}\right]+c.c. \tag{4.27}$$

As we can see above, the ρE_2 term is driving for the field $\tilde{E}_1$, and the ρ^*E_1 term for the field $\tilde{E}_2$. If the fields in the form of eq. (4.1) is inserted in eq. (4.23) and evaluated, the result becomes a complicated equation with 12 different terms. It can however be simplified if we apply the slowly-varying-amplitude approximation, and drop the second derivatives. This can be done if the envelope of the field varies much slower than the field oscillates. At 532 nm, the period of the oscillating field is 2.4 fm, which is 10^6 times shorter than the duration of the pulse from the Nd:YAG laser discussed.

The approximation leads to the following equations

$$\frac{\partial}{\partial z}E_1 + \frac{n}{c}\frac{\partial}{\partial t}E_1 = \frac{i\mu c\omega_1\gamma_e}{4n\rho_0}\left(\rho E_2 + \frac{2i}{\omega_1}\frac{\partial}{\partial t}(\rho E_2)\right) \tag{4.28a}$$

and

$$-\frac{\partial}{\partial z}E_2 + \frac{n}{c}\frac{\partial}{\partial t}E_2 = \frac{i\mu c\omega_2\gamma_e}{4n\rho_0}\left(\rho^* E_1 + \frac{2i}{\omega_2}\frac{\partial}{\partial t}(\rho^* E_1)\right) \tag{4.28b}$$

Since ω_1 and ω_2 are very large numbers, we can do another approximation by omitting the second terms to the right. After this, we have reached the final form of the wave equations.

$$\frac{\partial}{\partial z}E_1 + \frac{n}{c}\frac{\partial}{\partial t}E_1 = \frac{i\mu c\omega_1\gamma_e}{4n\rho_0}\rho E_2 \tag{4.29a}$$

$$-\frac{\partial}{\partial z}E_2 + \frac{n}{c}\frac{\partial}{\partial t}E_2 = \frac{i\mu c\omega_2\gamma_e}{4n\rho_0}\rho^* E_1 \tag{4.29b}$$

We now need to describe how the density wave is driven by the field amplitudes. The behaviour of acoustic waves is well known, and we begin by writing down the acoustic wave equation in one dimension [10]

$$\frac{\partial^2}{\partial t^2}\tilde{\rho} - v^2\frac{\partial^2}{\partial z^2}\tilde{\rho} - \Gamma\frac{\partial^3}{\partial z^2\partial t}\tilde{\rho} = 0 \tag{4.30}$$

where the damping parameter Γ can be expressed as

$$\Gamma = \frac{1}{\rho_0}\left(\frac{4}{3}\eta_s + \eta_b + \kappa\left(\frac{1}{C_p} - \frac{1}{C_v}\right)\right) \tag{4.31}$$

η_s and η_b are the shear and bulk viscosity coefficients, κ is the thermal conductivity, C_p and C_V are specific heat of constant pressure and volume respectively. To understand the physical meaning of the damping parameter, we consider a acoustic field of the form

$$\tilde{\rho}(z,t) = \rho_0(0,t)e^{i(qz-\Omega t)} \tag{4.32}$$

at steady state conditions, i.e. $\frac{\partial\rho_0}{\partial t} = 0$. If this expression is inserted in the acoustic wave equation, we get the relation

$$-\Omega^2 + v^2q^2 - iq^2\Omega\Gamma = 0 \tag{4.33}$$

Then, if q is approximated with

$$q \approx \frac{\Omega}{v} + \frac{iq^2\Gamma}{2v} \tag{4.34}$$

the intensity of the acoustic wave will be expressible as

$$\left|\tilde{\rho}(z,t)\right|^2 = \left|\rho(0,t)\right|^2 \left| e^{i\left(\frac{\Omega}{v}z + \frac{iq^2\Gamma}{2v}z - \Omega t\right)} \right|^2 = \left|\rho(0,t)\right|^2 e^{-\frac{q^2\Gamma}{v}z} \tag{4.35}$$

This is how the acoustic wave will be attenuated as it propagates in the medium. We define the phonon lifetime according to

$$\tau_p = \frac{1}{q^2\Gamma} \tag{4.36}$$

The corresponding phonon decay distance will be

$$L_p = \frac{v}{q^2\Gamma} \tag{4.37}$$

This is of crucial importance, since the minimum laser-pulse duration due to SBS will be of the same order of magnitude as

$$\tau_{min} = \frac{nL_p}{c} = \frac{nv}{q^2\Gamma c} \tag{4.38}$$

In table 4-1, this quantity is shown for different liquids at 532nm.

Liquid	τ_{min} [7] [ps]
Water	295
Methanol	374
CCl_4	144

Table 4-1

To obtain waves in the medium, we add a source term to eq (4.30). As such, we have the divergence of the force per unit volume.

$$f = \nabla p \tag{4.39}$$

there p is the pressure from eq. (4.16).

The electric field in eq. (4.16) is the sum of the incident and the reflected wave. In the squared expression there is a term that can act as source of the acoustic wave. The force per unit volume is then (in one dimension)

$$f = -\frac{1}{2}\gamma_e \frac{\partial}{\partial z}\left(E_1 E_2^* e^{i(qz-\Omega t)}\right) + c.c. \tag{4.40}$$

The source term is the divergence of this. We get

$$\frac{\partial}{\partial z}\left[-\frac{1}{2}\gamma_e \frac{\partial}{\partial z}\left(E_1 E_2^* e^{i(qz-\Omega t)}\right) + c.c.\right] = \gamma_e E_1 E_2^* q^2 e^{i(qz-\Omega t)} + c.c. \tag{4.41}$$

Now we insert eq. (4.2) in the acoustic wave equation, and apply the slowly varying amplitude approximation. If we also insert the source term, we have

$$\frac{1}{2}\left(-2i\Omega\frac{\partial}{\partial t}\rho - i\Omega q^2\Gamma\rho - 2iqv^2\frac{\partial}{\partial z}\rho\right) = \gamma_e E_1 E_2^* q^2 \tag{4.42}$$

which we rewrite as

$$\Omega q^2\Gamma\rho + 2qv^2\frac{\partial}{\partial z}\rho + 2\Omega\frac{\partial}{\partial t}\rho = 2i\gamma_e E_1 E_2^* q^2 \tag{4.43}$$

4.3.3 Threshold Intensity

The three equations ruling the SBS-process are

$$\frac{\partial}{\partial z}E_1 + \frac{n}{c}\frac{\partial}{\partial t}E_1 = \frac{i\mu c\omega_1\gamma_e}{4n\rho_0}\rho E_2 \tag{4.44}$$

$$-\frac{\partial}{\partial z}E_2 + \frac{n}{c}\frac{\partial}{\partial t}E_2 = \frac{i\mu c\omega_2\gamma_e}{4n\rho_0}\rho^* E_1 \tag{4.45}$$

$$\Omega q^2\Gamma\rho + 2qv^2\frac{\partial}{\partial z}\rho + 2\Omega\frac{\partial}{\partial t}\rho = 2i\gamma_e E_1 E_2^* q^2 \tag{4.46}$$

By neglecting the motion of the acoustic wave while the light passes, we can reduce the equations to

$$\frac{\partial}{\partial z}E_1 + \frac{n}{c}\frac{\partial}{\partial t}E_1 = -\frac{\mu c\omega_1\gamma_e^2}{2n\rho_0\Omega\Gamma}E_1 E_2 E_2^* \tag{4.47a}$$

$$-\frac{\partial}{\partial z}E_2 + \frac{n}{c}\frac{\partial}{\partial t}E_2 = \frac{\mu c\omega_2\gamma_e^2}{2n\rho\Omega_0\Gamma}E_1 E_1^* E_2 \tag{4.47b}$$

To find the equations for the intensities instead of the fields, we first multiply with E_1^* in eq. (4.47a) and E_2^* in eq. (4.47b). Thereafter we add the equations with their complex conjugates. Then we have

$$\frac{\partial E_1}{\partial z}E_1^* + \frac{\partial E_1^*}{\partial z}E_1 + \frac{n}{c}\left(\frac{\partial E_1}{\partial t}E_1^* + \frac{\partial E_1^*}{\partial t}E_1\right) = -\frac{\mu c\omega_1\gamma_e^2}{n\rho_0\Omega\Gamma}E_1E_1^*E_2E_2^* \quad (4.48a)$$

and

$$-\left(\frac{\partial E_2}{\partial z}E_2^* + \frac{\partial E_2^*}{\partial z}E_2\right) + \frac{n}{c}\left(\frac{\partial E_2}{\partial t}E_2^* + \frac{\partial E_2^*}{\partial t}E_2\right) = \frac{\mu c\omega_2\gamma_e^2}{n\rho_0\Omega\Gamma}E_1E_1^*E_2E_2^* \quad (4.48b)$$

The intensity of a field written on the form of eq. (4.1) is

$$I_i = \frac{\varepsilon}{2}\frac{c}{n}E_iE_i^* \quad (4.49)$$

If we write $\omega_1 = \omega_2 = \omega$, the final equations become

$$\frac{\partial I_1}{\partial z} + \frac{n}{c}\frac{\partial I_1}{\partial t} = -gI_1I_2 \quad (4.50a)$$

and

$$\frac{\partial I_2}{\partial z} - \frac{n}{c}\frac{\partial I_2}{\partial t} = -gI_1I_2 \quad (4.50b)$$

Here we have introduced the Brillouin gain constant g, according to

$$g = \frac{\mu\omega\gamma_e^2}{\varepsilon\rho_0\Omega\Gamma} \quad (4.51)$$

In table 4-2, g is given for some different liquids.

Liquid	g [4] [cm/MW]
Water	0.0048
Methanol	0.013
CCl_4	0.006

Table 4-2

Below the threshold for SBS, we have a steady state in case of a continuos incident wave. This means that

$$\frac{\partial I_1}{\partial z} = \frac{\partial I_2}{\partial z} \quad (4.52)$$

and

$$I_1(z) = I_2(z) + C \quad (4.53)$$

where C depends on the boundary conditions.

Far below the threshold, the intensity of I_1 does not change very much and can be considered constant. I_2 then obeys

$$\frac{\partial I_2(z)}{\partial z} = -gI_1 I_2(z) \tag{4.54}$$

The solution is (with L as the length of the interacting region)

$$I_2(0) = I_2(L)e^{gI_1 L} \tag{4.55}$$

Since the SBS-process is initiated by spontaneous scattering, we can assume that I_2 is proportional to I_1 at the far end of the interacting region.

$$I_2(L) = KI_1(L) \approx KI_1(0) \tag{4.56}$$

leading to

$$I_2(0) = I_1(0)Ke^{gI_1 L} \tag{4.57}$$

This is the behaviour at low intensities. We define the SBS-threshold as the intensity needed for the reflectivity to be unity. Then

$$gI_1 L \geq \ln\left(\frac{1}{K}\right) \tag{4.58}$$

Laboratory experience has shown that gI_2L is approximately 30 for most materials. A test with the preliminary set-up, with a beam travelling L=150 cm in water showed no SBS at 300 mJ. Since it is difficult to vary the laser energy in small steps with the external control device, exact values are hard to obtain, but at 550 mJ there was significant SBS. The beam diameter was 12.7 mm and the pulse length 7.5 ns. With g=0.0048 cm/MW for water, we get the lower and upper bounds for gI_1L to be

$$21 \leq gI_1 L \leq 39 \tag{4.59}$$

This result fits well into the theory.

4.3.4 Above the Threshold

As the power rise above the threshold, many of our recent approximations fail. The pulse will still initiate on spontaneous scattering, and it will increase in magnitude exponentially. When the intensity of the scattered wave has reached that of the incident, the pulse will start to compress. A side effect of this is that the peak power continues to increase. This goes on until the pulse length is as long (or rather as short) as the phonon decay distance. There are different opinions what the theoretically shortest pulse width is. The first theory was that

$\tau_{SBS} \approx \tau_{min}$ from eq [4.38], but since then estimates such as $\tau_{SBS} \approx 0.1\tau_{min}$ and $\tau_{SBS} \propto \sqrt{\tau_{min}}$ have been made[7].

4.4 Phase Conjugation of the Scattered Beam

Whenever a beam of high intensity is focused in some medium, backscattering can occur. Apart from Brillouin there are several processes (e.g. Raman, Rayleigh, Rayleigh-wing) which all have one thing in common; the back-scattered wave is phase conjugated. Phase conjugation is a kind of reflection, which differs o lot from ordinary reflection (figure 4-2). There are several variants, but in the case of stimulated back scattering, we have spatial phase conjugation, or wave front reversal. The wave "turns" and goes back the same way as it came. The polarization state behaves however as in normal mirror reflection [13].

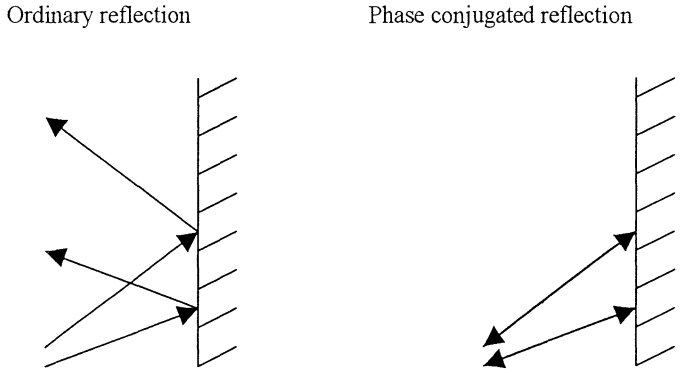

Figure 4-2 Phase conjugated reflection.

The phase conjugation is a "good" effect apart from most of those described below. It makes the design extremely stable. A large displacement (1 cm) of a mirror in the set-up would normally ruin the alignment, but all we have to do is to direct the beam into the cells again. Once we have a focus, the beam will nicely return exactly along the same path as it came.

Distortions in the beam will also disappear due to the phase conjugation. In figure 4-3, we can see how the disturbances due to diffraction disappears after that the wave travels back to the laser.

4.5 Other Nonlinear Effects

The main difficulty in SBS pulse compression is not to obtain SBS-radiation, which is very easy. It is rather to minimise all other disturbing nonlinear effects. The three largest is dielectric breakdown in the Brillouin medium, stimulated Raman scattering and diffuse Brillouin scattering.

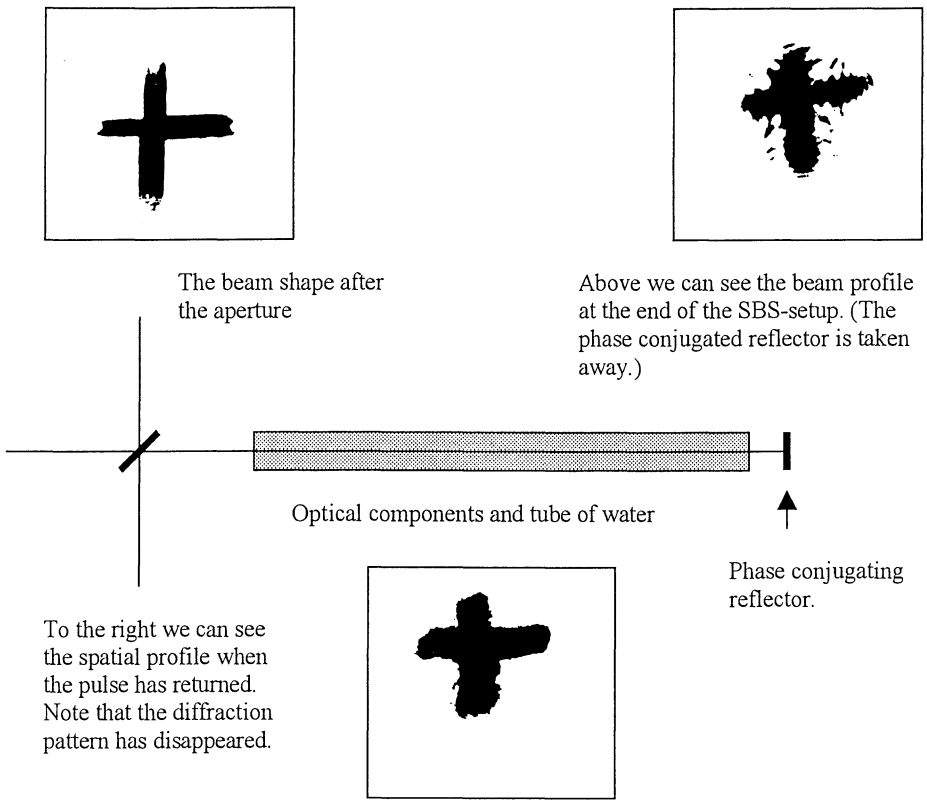

Figure 4-3 Elimination of disturbances along the beam path due to phase conjugation.

4.5.1 Laser Induced Breakdown in the Focused Beam

If a material is exposed to a sufficiently high electric field, the material will break down and form a plasma. In case of laser radiation, a high intensity beam can cause breakdown if focused, and since we want the SBS process, we depend on the focusing of the beam. There is no risk for breakdown in the beam unless we focus it.

If a breakdown occur, we can observe it as a small flash of light (see figure 4-4), originating from Bremsstrahlung emission and recombination of electrons. The high pressure and temperature in the plasma will cause it to expand, vaporising more liquid and create a supersonic shock wave, which can be heard as a loud "crack". The vaporised liquid will expand and form a small cavitation bubble, which may or may not collapse and reexpand a number of times. After a while this process will stabilise, and we can then observe the residual bubble, moving away from the focus with high speed. Within about ten millimetres, it will slow down and come to rest in the liquid.

The breakdown process starts when a free electron absorbs photons from the field, and is accelerated. It will create more free electrons by collision ionisation, which in turn will be accelerated. Within soon we will have an avalanche of accelerating electrons, and when the electron density has risen to

10^{18} –10^{20} cm^{-3} breakdown occurs. This kind of breakdown process is called "avalanche ionisation breakdown". The first free seed-electron can either be a quasi-free electron from an impurity in the liquid or created by multi-photon ionisation. For our pulse widths and energies, impurity initiation is the primary cause of breakdown events.

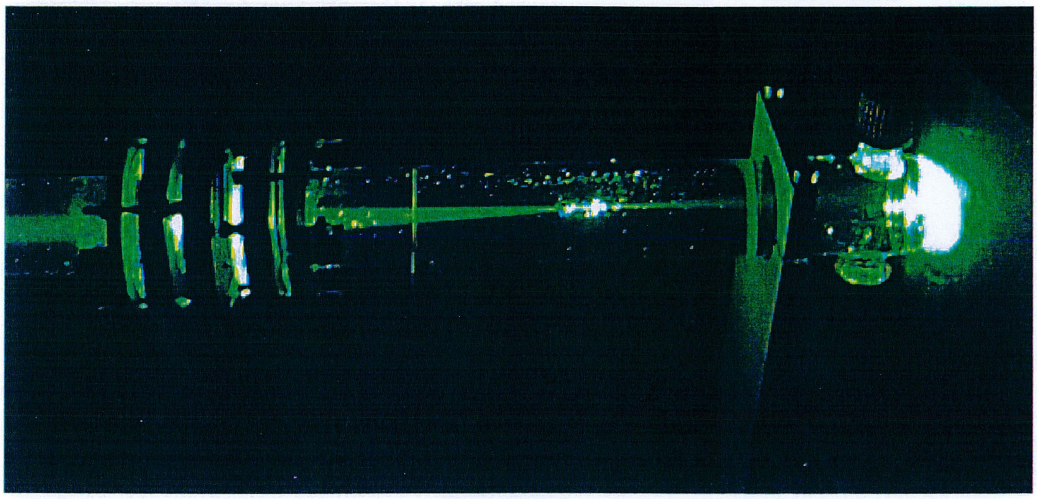

Figure 4-4 Breakdown in water. We can see the laser beam leave the amplifier cell, and enter the oscillator in the right part of the picture. Between the cells is a lens, and in the middle of the picture (in the focus of the lens), we can see a flash of light caused by the breakdown.

It is easy to compute the highest intensity in the focal beam waist. We have a near top-hat spatial profile as output from the Nd:YAG laser. The beam has a diameter of 9 mm (=2R) and is focused by a 130 mm (=f) lens, the area of the beam waist is then

$$A = \pi r^2 = \pi\left(\frac{\lambda f}{\pi R}\right)^2 \approx 7.5 \cdot 10^{-7}\,cm^2 \qquad (4.60)$$

There is no distinct threshold intensity, since the breakdown event is triggered by fluctuations in the liquid. For estimating, we will use the value of 9 x 10^9 W/cm^2 for 50% risk of breakdown [14]. Then the highest allowed power of the pulse will be

$$P = I \cdot A \approx 6.8\,kW \qquad (4.61)$$

This corresponds to a pulse energy of only 54 μJ (FWHM 7.5 ns). Under normal operation with the SBS-compressor, most of the power in the pulse will be reflected. However, if the seeding unit is not working properly, the SBS will not occur, meaning that the much higher intensity in the middle of the pulse will reach the focal region of the lens. Since the Nd:YAG laser operates in the 100 mJ-region, this will causing breakdown practically all the time.

The probability that breakdown events should occur is, as said before, greatly enhanced by impurities in the medium. Figure 4-4 shows the focus of the beam in the generator cell. To the left, the power is to low for breakdown,

but in the focus it is sufficient. To minimise the risk of breakdown, very clean water must be used. The cell must be made of a material that does not pollute the water, and the water must be easy to replace in case of pollution. By heating and filtering the (already distilled) water before it is poured into the cell, the threshold for breakdown can be raised.

The breakdown in the liquid will result in gas bubbles, which by themselves can initiate other breakdowns. The result is that the liquid rather quickly, as can be seen in figure 4-5, is filled with bubbles. This problem is not that serious, since the bubbles will disappear as soon as one let the water rest. By heating and filtering the (already destined) water before it is poured into the cell, the threshold for breakdown can be raised.

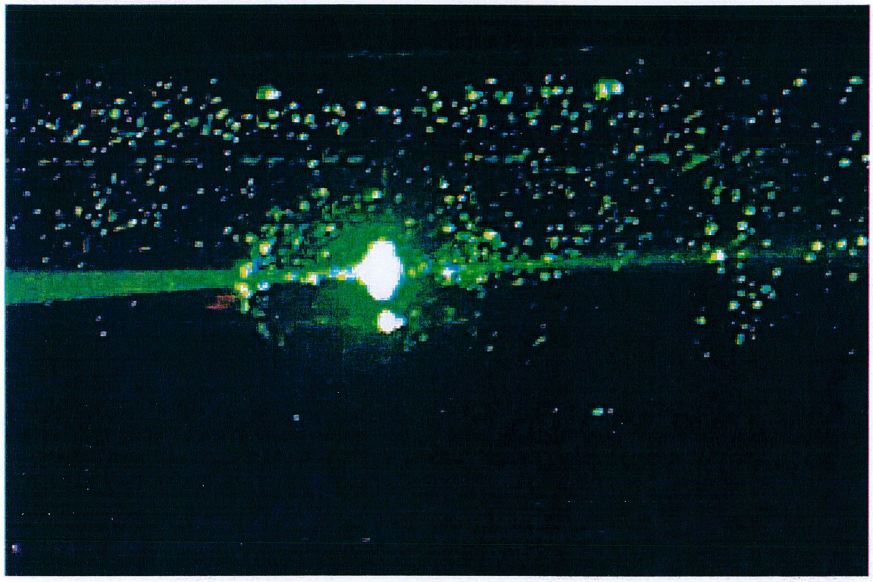

Figure 4-5 Close up on breakdown in water.

4.5.2 Stimulated Raman Scattering

A nonlinear process, competitive with SBS is stimulated Raman scattering (which will be written SRS from now on). Raman scattering is the scattering from optical phonons instead of acoustic, and the theory behind the mechanism is well known (see figure 4-6). The light excites the molecule of the medium to a virtual energy level. When relaxation occurs, the molecule ends up in a state with slightly higher energy than the ground state. The scattered light will therefore have less energy (longer wavelength) than the original beam. Since a small fraction of the molecules in the liquid already is in a higher state due to statistic fluctuations, the reversed process can also occur. Then the molecules ends up in a state with lower energy than the initial one and we get scattered light with a higher energy (shorter wavelength). The scattered light with lower energy than the incident is called stokes-shifted, and that with higher, anti-stokes-shifted.

The process of SRS is very similar to SBS, and the efficiency will rise quickly for higher intensities of the light once the threshold is reached. When this process gains strength, it becomes harder to increase the power of the Brillouin shifted beam.

It is easy to observe the effect in the SBS-compressor. The Raman shift is much larger than the Brillouin shift and since the dielectric mirrors in the design are optimised for 532nm, a large fraction of the Raman shifted light goes through them. Both the stokes and anti-stokes components of the SRS can easily be seen on a screen placed behind a mirror.

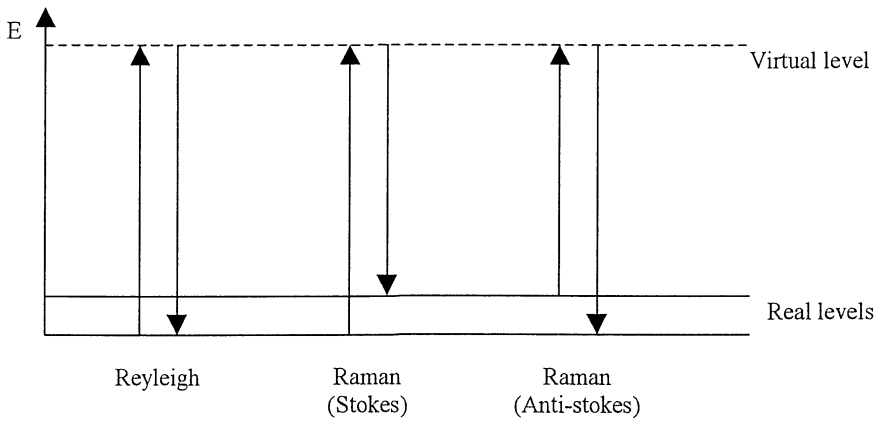

Figure 4-6 Raman and Rayleigh scattering

SRS-initiation in the focus is highly enhanced by spatial irregularities in the beam. This could be seen in one of the early designs, when there were small damages in the optics. The part of the beam that went through a small burn mark in the entrance window of the cell, glowed red in the water before the rest of the beam.

4.5.3 Diffuse Brillouin Scattering

The phase conjugation of the beam takes place in the focus. If the beam energy is high enough, SBS can occur before the focus, resulting in back scattered which is not phase conjugated. This can be seen as a small pre-pulse before the main pulse if the compressed pulse is studied on an oscilloscope. This effect is not only a drawback, since a small amount of diffuse Brillouin scattering results in a remarkable higher compression ratio, but it sets a limit for the maximum power of a beam with a given radius. If a beam expander is used, the maximum power can be higher, but the compression ratio decrease. Another way to obtain higher energies is to choose a medium with a lower Brillouin-gain constant.

5 Development of an SBS-Compressor

The first question was where in the VUV generation set-up we should put the compressor. The most important factor that limits our freedom of choice is the bandwidth of the laser. As we know, the process of stimulated Brillouin scattering is initiated by the interference between the original beam and spontaneous scattering. The bandwidth of the laser must therefore be smaller than the Brillouin bandwidth, and the only beam which matches this criterion is the one from the seeded Nd:YAG laser [3].

We need to take the beam from the Nd:YAG laser, send it through an SBS-compressor, and lead it into the dye laser. Since the compressed pulse will be phase conjugated, and hence reflected back exactly the same way, we need to prevent it from returning into the Nd:YAG laser and causing damage. This can be accomplished by a combination of a quarter-wave plate and a polarization device (see figure 5-1 for layout). However, in this way the plane of polarization is rotated 90°. The original beam is vertically polarized, and since the input beam to the dye laser also must be that, we will have to rotate the polarization of the beam back to vertical. This we can do with a combination of mirrors or with a half wave plate.

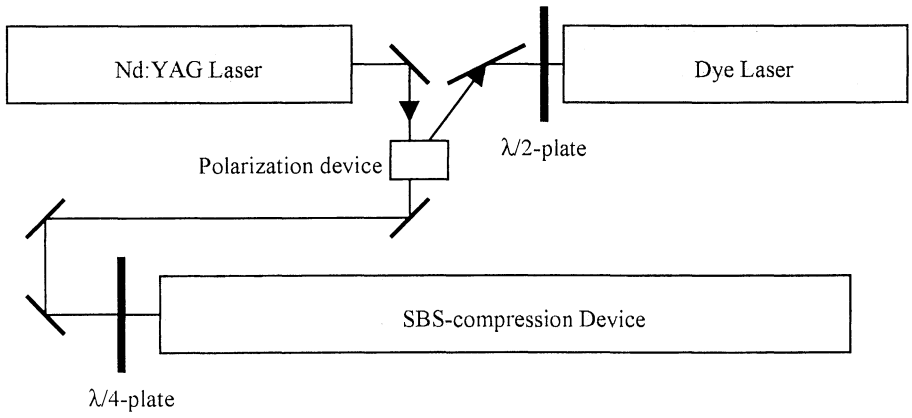

Figure 5-1 Layout of the placement of the SBS-compressor in the laser system.

5.1 Choice of Design

In the literature one find that there are in fact several possible ways to obtain an SBS-compressed pulse. An early method was with tapered waveguides [15]. Focusing lenses with long focal lengths makes thing easier, but the SBS threshold is reached too soon. For higher power, a two-cell design is better [7], and for very high power, a small fraction of the beam can be used as a seeder [9]. The different designs can be seen in figure 5-2.

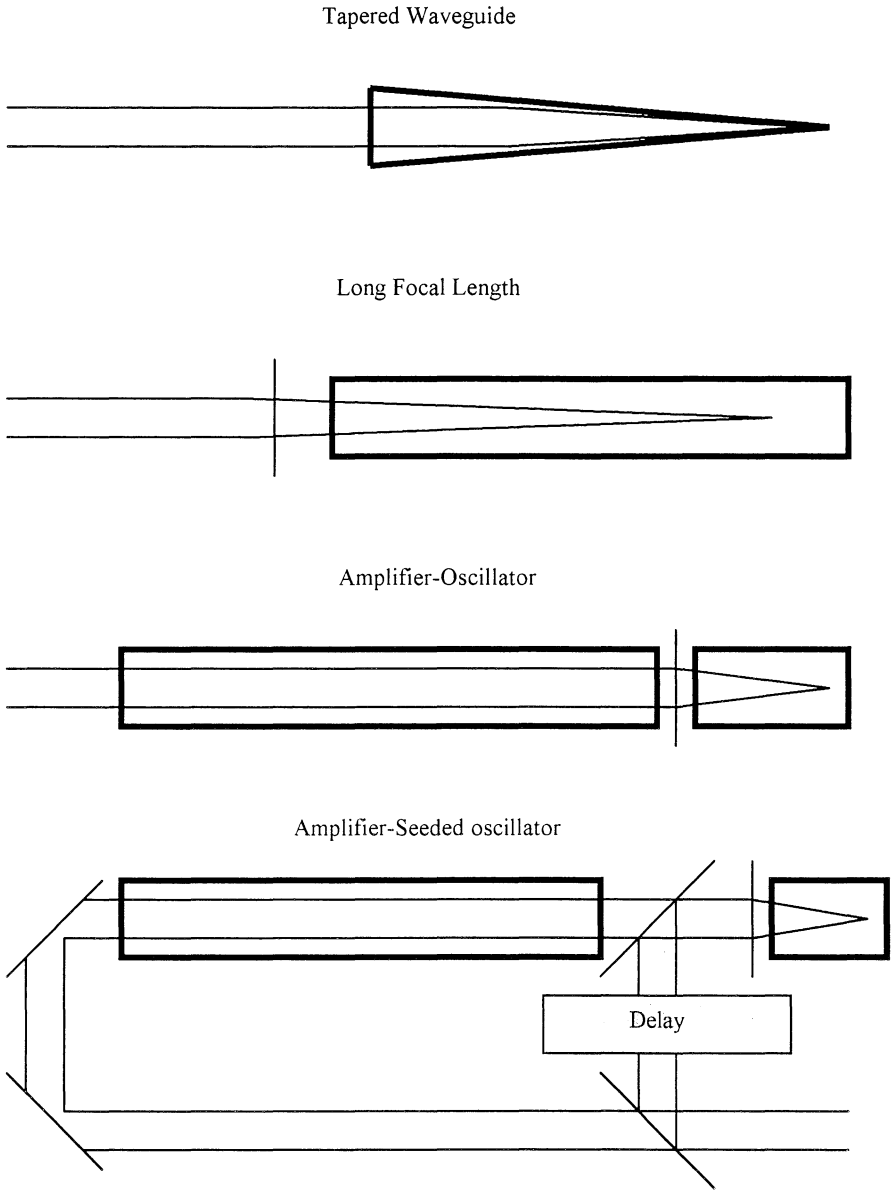

Figure 5-2 Different SBS-compressor designs. In the tapered waveguide, the intensity gets higher as the light follows the walls of the cell. In the other three designs, focusing lenses are used to obtain sufficiently high intensity. In the last design, a small fraction of the energy of the beam is used to start the SBS-process.

5.2 The First model

The design with a long amplifier cell and a shorter oscillator was found to be suitable for our pulse energies end therefore chosen. There were three phases in the development of the compressor. First, an experimental set-up with metal

water cells was made in a laboratory adjacent to the Nd:YAG laser. In this stage only uncoated optics were used, and the compressed pulse was not sent back to the dye laser. After that, the compressor was moved into the same room as the laser, the plate polarizers were put in (see 5.3.2) and coated optics was used. Finally, the metal cells were replaced with glass ones, and the whole design was mounted permanently on the optic table of the VUV-laser system.

5.2.1 Choice of Brillouin Medium

In principle, any transparent medium could serve as a Brillouin scatterer. Crystals are very expensive and have a tendency to be damaged by dielectric breakdown, and gases must be kept under high pressure to be useful. Therefore, liquids are the best choice for a simple and cheep design. Since it is favourable with a small beam radius, the choice is limited to media with low Brillouin gain. It is also preferable that the media should be non-poisonous and non-flammable.

Since water fills all the set demands, and also is highly transparent at 532 nm, it was the obvious choice. Other liquids with low Brillouin gain are methanol and carbontetracloride. Both are easier to keep clean since the risk of algae growth disappears, but since methanol could be explosive if the containers should leak, and carbontetracloride is highly poisonous, water was preferred.

5.2.2 Design

The first model was a set of steel cells with attachable windows on the ends (figure 5-3 and 5-4). The Amplifier was made of two tubes of different diameter, which were made to fit into each other. By moving the smaller one, the length of the tube could be varied from 100 to 160 cm. A hose from a container filled with distilled and deionised water, was attached to a nozzle near the end of the larger tube. When the length of the cell was to be adjusted, the water could flow freely in and out of it. The oscillator cell was of similar design as the amplifier, but only 30 cm long. Between the cells was a focusing lens with a focal length of 10 cm. Since the beam after the lens enters the water filled oscillator cell, the effective focal length becomes about 30% longer.

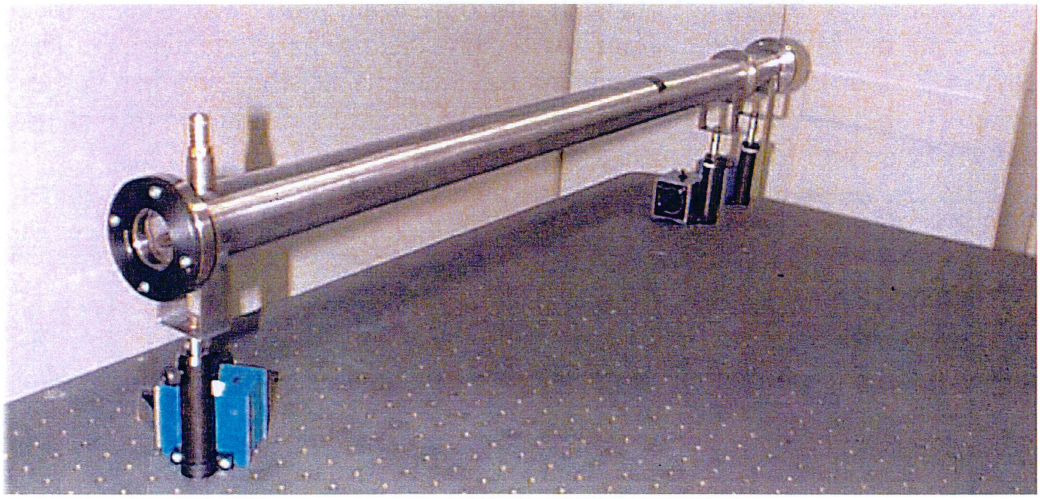

Figure 5-3 First model, amplifier cell

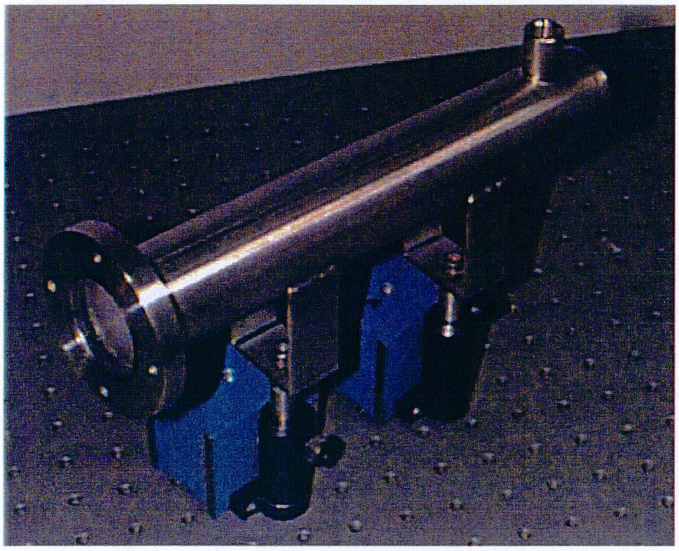

Figure 5-4 First model, Oscillator cell.

To separate the original beam from the reflected, a Glan-laser prism in combination with a quarter wave plate was used. Such prisms give a high degree of polarization purity of the transmitted and reflected light, but are rather sensitive to high intensities. (Unfortunately, the first Glan-laser prism was destroyed when a mirror burned and caused hotspots in the beam.)

Between the wave plate and the prism, a beamsplitter was inserted, with which a portion of the compressed pulse could be observed. Since the ratio between reflected and transmitted light in the beamsplitter was known, the energy of the compressed pulse could be calculated. By putting in a photo-diode connected to an oscilloscope with large bandwidth, it was also possible to measure the duration of the pulse with this design.

5.2.3 Distortion of the Beam Profile

According to the literature, one important issue for reaching a high Brillouin efficiency is a good spatial profile of the beam. If the beam that is to be compressed has a Gaussian profile, it will not be distorted when it propagates. The Gaussian profile is, unfortunately, the only beam profile with such a nice behaviour, and all deviations from it will cause distortions after a distance. The Nd:YAG laser is lasing uniformly in the whole YAG-rod, and has consequently a top hat beam profile. The theory of Fraunhofer diffraction then states that the beam profile will change as it propagates.

This can be seen with help of burn marks made on light sensitive paper placed at different distances from the laser (figure 5-5). Note how the edges of the distortion in the right of the beam are changing when the pulse propagates.

Additional disturbances in the beam (dust on mirrors, apertures, etc) will also aggravate as the pulse travels. Apart from lowering the Brillouin efficiency and compression ratio, this can cause damage in the optics.

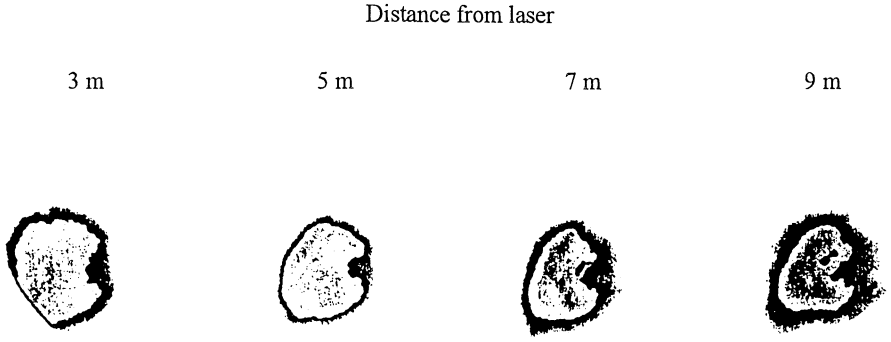

Figure 5-5 Distortion of the beam profile due to propagation.

To prevent damages and to get a high efficiency of the process, it is important that the beam profile is sufficiently good at the entrance of the amplifier cell. This can be achieved in several ways. A simple method is to put a spatial filter somewhere in the beam. This will result in a beam with a near Gaussian profile, but since spatial filtering means that the beam is focused, this must be done in vacuum. The spatial filter absorbs the spatial frequencies which does not fit in the Gaussian profile, which means we lose power. It is also better to maintain the top-hat profile in the medium, since the temporal profile of the scattered light then will be the same in all parts of it. (If the intensity should be lower in one part of the beam, then the threshold for SBS would be reached later.)

Another way to minimise distortions is to image the exit side of the YAG-rod onto the entrance window of the amplifier cell, which can be done with a pair of lenses. This also includes a vacuum system but is apart from this an efficient method.

The simplest way to overcome the problems of propagation is to minimise the distance the light has to travel. The first compressor was built in a room adjacent to the VUV-laboratory. Since the distance to the laser was then almost ten metres, the beam profile was extremely bad. When the compressor was moved into the same room as the laser, the profile was considerable better, and so were the results.

The final design is mounted next to the laser, with only 150 cm path length from the laser to the entrance of the SBS tube.

5.3 Final design

5.3.1 Tube Material and Length

One of the biggest problems with the first design, was that the water so quickly became polluted. A metal surface is always porous to some degree, and will contain traces of e.g. oil and corrosion products, which will dissolve in the water.

After only one or two days, the breakdowns in the water occurred so often, that measurements were impossible. For reliable results, one actually had to change water every day. To overcome this problem, the cells in the final design were made of glass. The water in these cells seems to keep clean. After one week, the breakdown threshold intensity had not changed.

To find the optimal tube length, measurement series were made with tube lengths of 150 cm, 130 cm and 110 cm. In figure 5-6, we can see how the pulse length and energy of the compressed pulse depends of this.

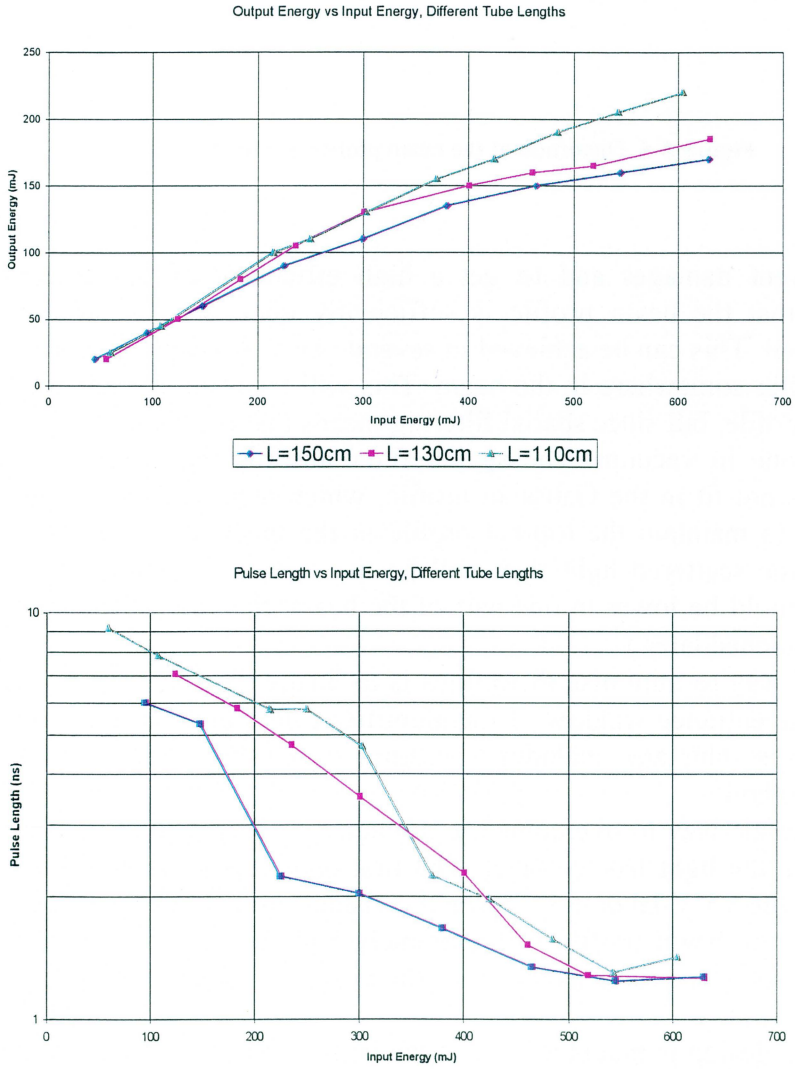

Figure 5-6 Tube length dependence of Output Energy and Pulse Length.

Clearly, a longer amplifier cell tends to give a better compression ratio but also lower efficiency. The upper limit to the output power is given by the damage threshold of the dye laser, and this power is much lower than the obtainable power from the compressor. Therefore, the amplifier was made as long as the optical table made possible, i.e. 150 cm.

5.3.2 The Polarizer

To separate the original from the compressed pulse, a construction with two coated glass plates was used instead of the Glan-laser prism (figure 5-7). Depending on the polarization state of the light, it can either be transmitted or reflected. Since the glass plates are mounted in the Brewster angle, they will automatically transmit all the horizontally polarized light, while the coating makes them reflect the vertically polarized. Each plate has en extinction ratio of 1:20, so by placing two in series, one obtains a ratio of 1:400. As the light from the Nd:YAG laser is frequency-doubled before it leaves the laser, there is no risk that the small amount of light that is reflected back into the cavity should cause any damage to the YAG crystal.

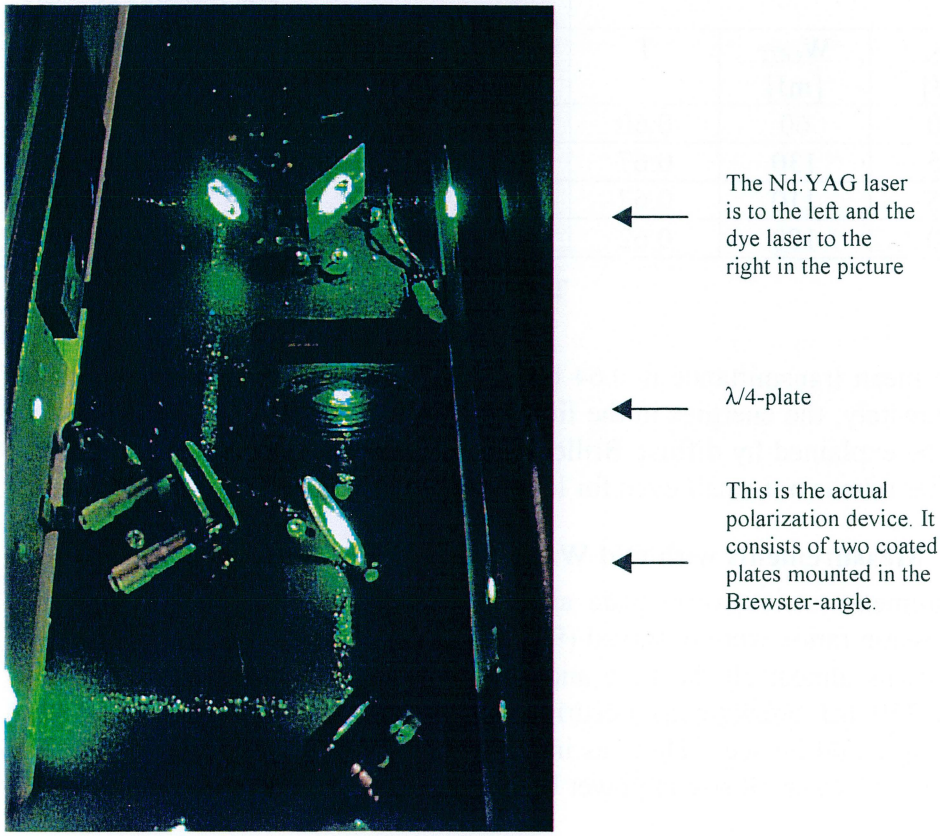

Figure 5-7 The Polarization device.

5.3.3 The Beam Expander

When the power is increased, the SBS-pulse changes appearance. For low energies, the pulse is partly compressed, but at a certain energy, there is a small rise in intensity before the sharp pulse arrives. At the same time, the sharpness of the peak increases (see fig 5-11)

This is what happens when the intensity of the incident light is so high that SBS starts spontaneously in the amplifier tube. The optimal energy from the YAG-laser should be just above this, to get the best compression. If the energy is increased even more, the pre-pulse will be stronger, draining energy from the peak.

5.4 Results

A variety of measurements has been done. When the pulse energy of the 532 nm radiation from the Nd:YAG laser is varied, this is done by turning the doubling crystal, since that does not alter the temporal profile of the pulse.

5.4.1 Losses in the Amplifier Tube

Measurements were made to determine the losses due to scattering in the amplifier tube. These were made with the metal tube, first with "old" water, and thereafter with "new" water.

Old water			New Water		
W_{IN} [mJ]	W_{OUT} [mJ]	T	W_{IN} [mJ]	W_{OUT} [mJ]	T
100	60	0.60	65	51	0.78
195	130	0.67	75	55	0.73
265	110	0.67	75	56	0.75
290	180	0.62	75	56	0.75

Table 5-1

The mean transmittance is 0.64 before and 0.75 after the change of water. Unfortunately, the energies in the first series are rather high, so the losses can partly be explained by diffuse Brillouin Scattering. However, the losses in the amplifier tube is not small even for low energies with new water.

5.4.2 Measurements with Old Water

Measurements series were made also with two days old water. Very good compression ratios were observed (940 ps, see figure 5-8), but then there were breakdowns almost all the time and the output pulses were highly unstable. Above 350 mJ breakdowns occurred most of the time, and strong Raman scattering could be seen. Here, as in all series, the diffuse Brillouin scattering can be seen as a small rise in power before the main pulse (figure 5-9).

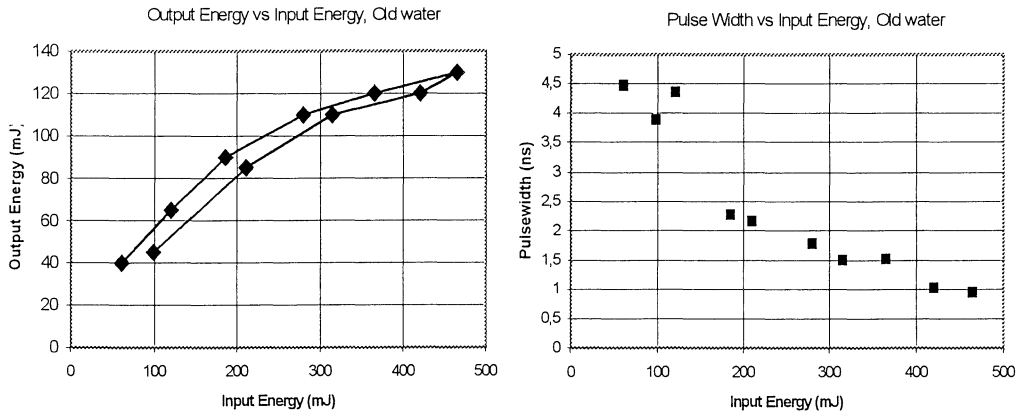

Figure 5-8 Pulsewidth and output energy for "old" water. Two series of measurement are shown in the figure.

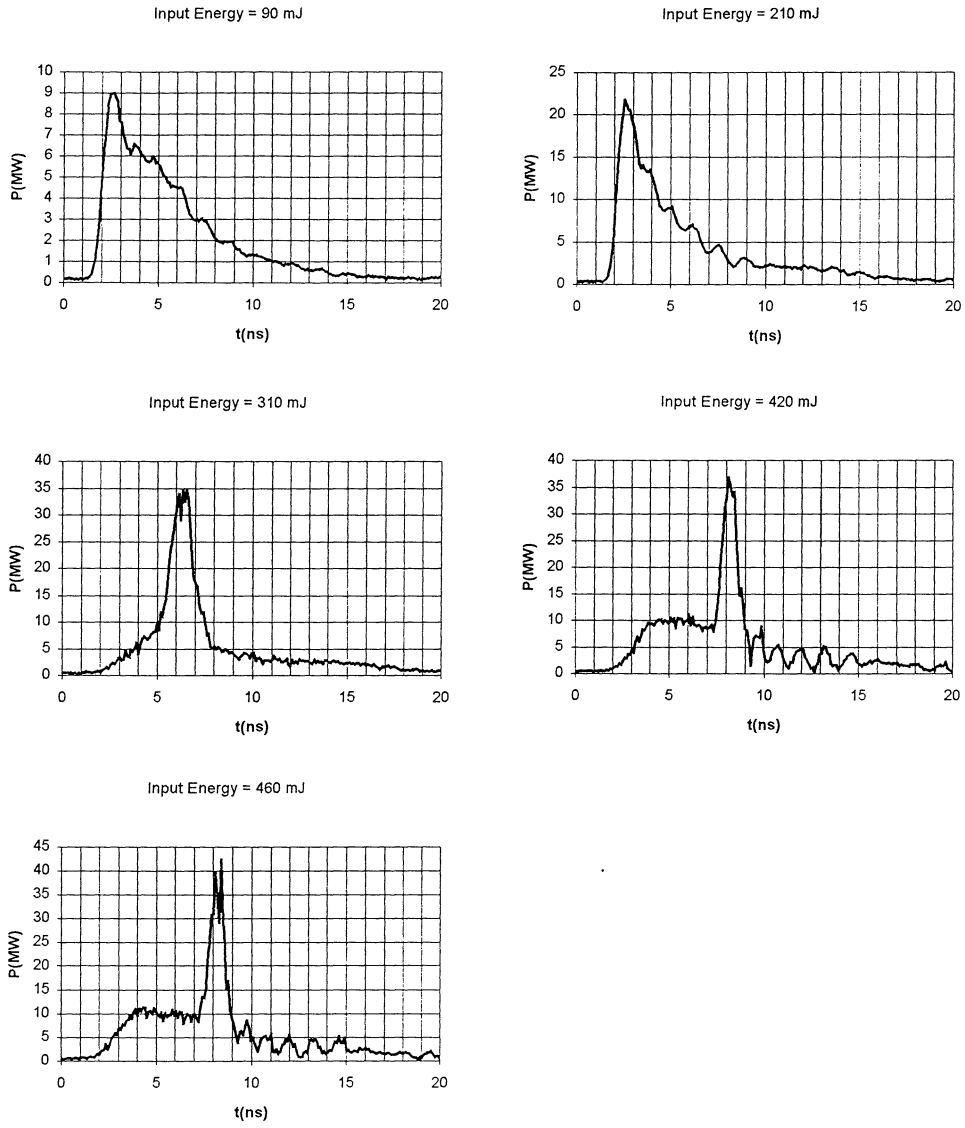

Figure 5-9 Pulseshapes for different energies, "old water". At 310 mJ, a small rise in intensity before the main pulse can be seen. This is due to diffuse Brillouin scattering in the amplifier cell.

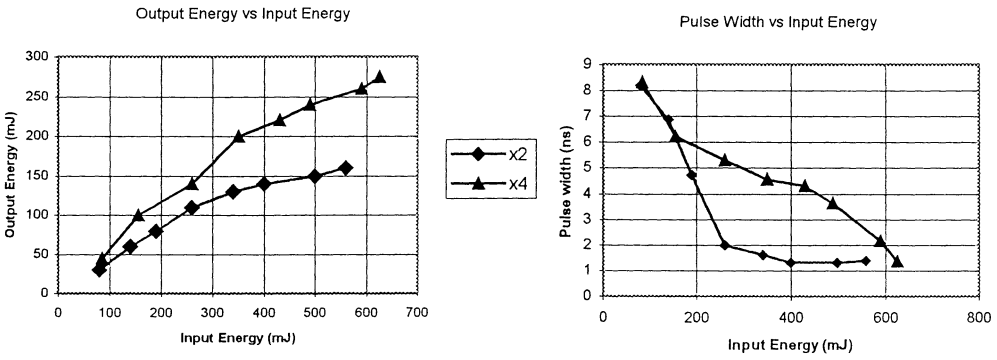

Figure 5-10 Pulse energy and width for two different beam-expanders. One of which expands the cross-section of the beam a factor two and the other a factor four.

5.4.3 Insertion of the Beam Expanders

Two beam expanders were tested. The first expands the beam cross-section a factor two and the second a factor four. With the large beam area, very high power could be reached, but unfortunately, the compression ratio is lower (figure 5-10, 5-11, 5-12). In [7], this is discussed, and expected to be due to spherical aberrations in the focusing lens.

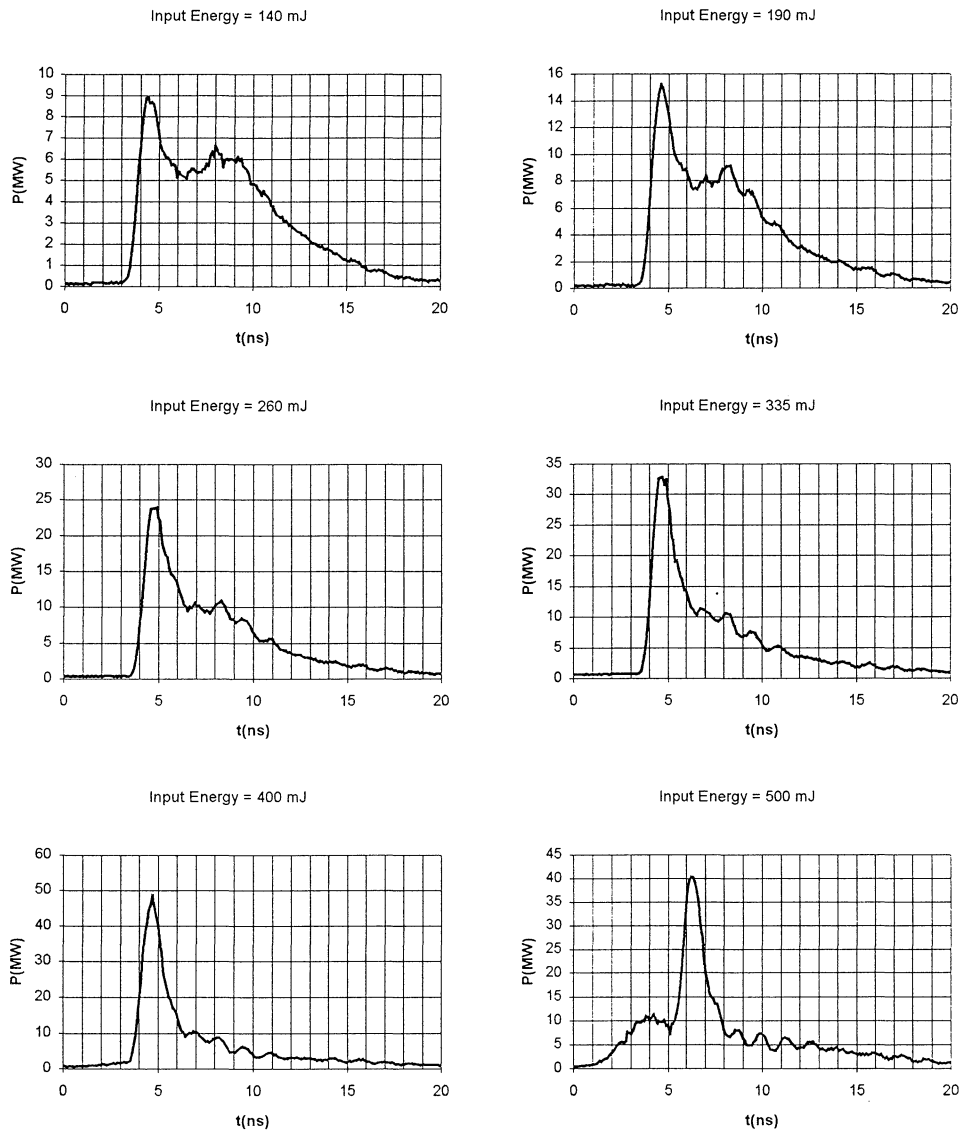

Figure 5-11 Pulse shapes for different energies. The diameter of the beam is 13 mm. The rise in power due to diffuse Brillouin scattering can be seen at 400 mJ. At 500 mJ this pre-pulse has become much stronger and begins to dominate over the main pulse, which has decreased in power.

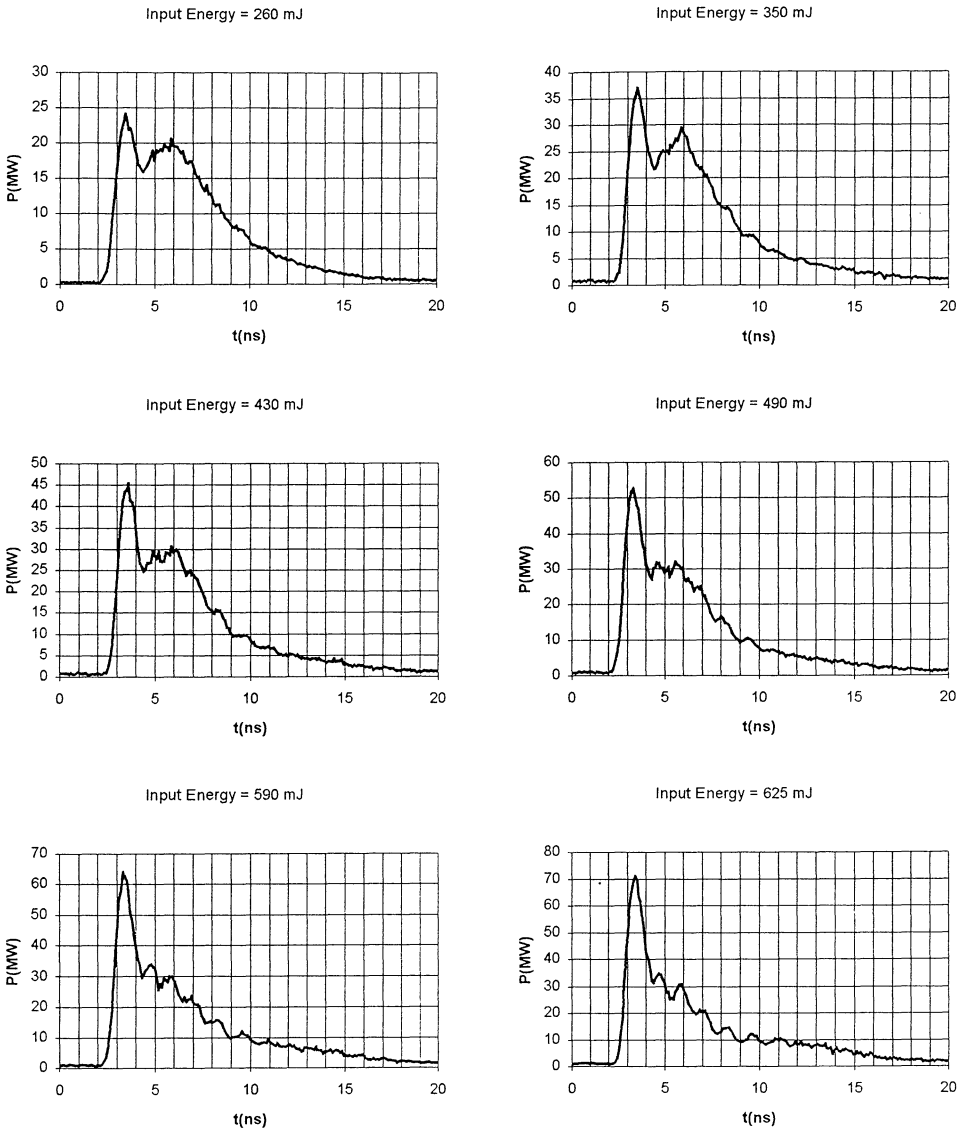

Figure 5-12 Pulse shape for different energies. The diameter of the beam is 18 mm. The beam cross-section is too large for diffuse Brillouin scattering to occur.

5.4.4 Dye Laser Output

The dye laser has an output of 10 to 15 mJ when pumped with the compressed pulse. The bandwidth has been measured with a wave meter and is stable at approximately 0.07 nm.

The following pictures were taken by a streak camera instead of a photo diode (figure 5-13), since the temporal resolution of streak cameras are much higher. The mean pulse width were measured to 740 ps.

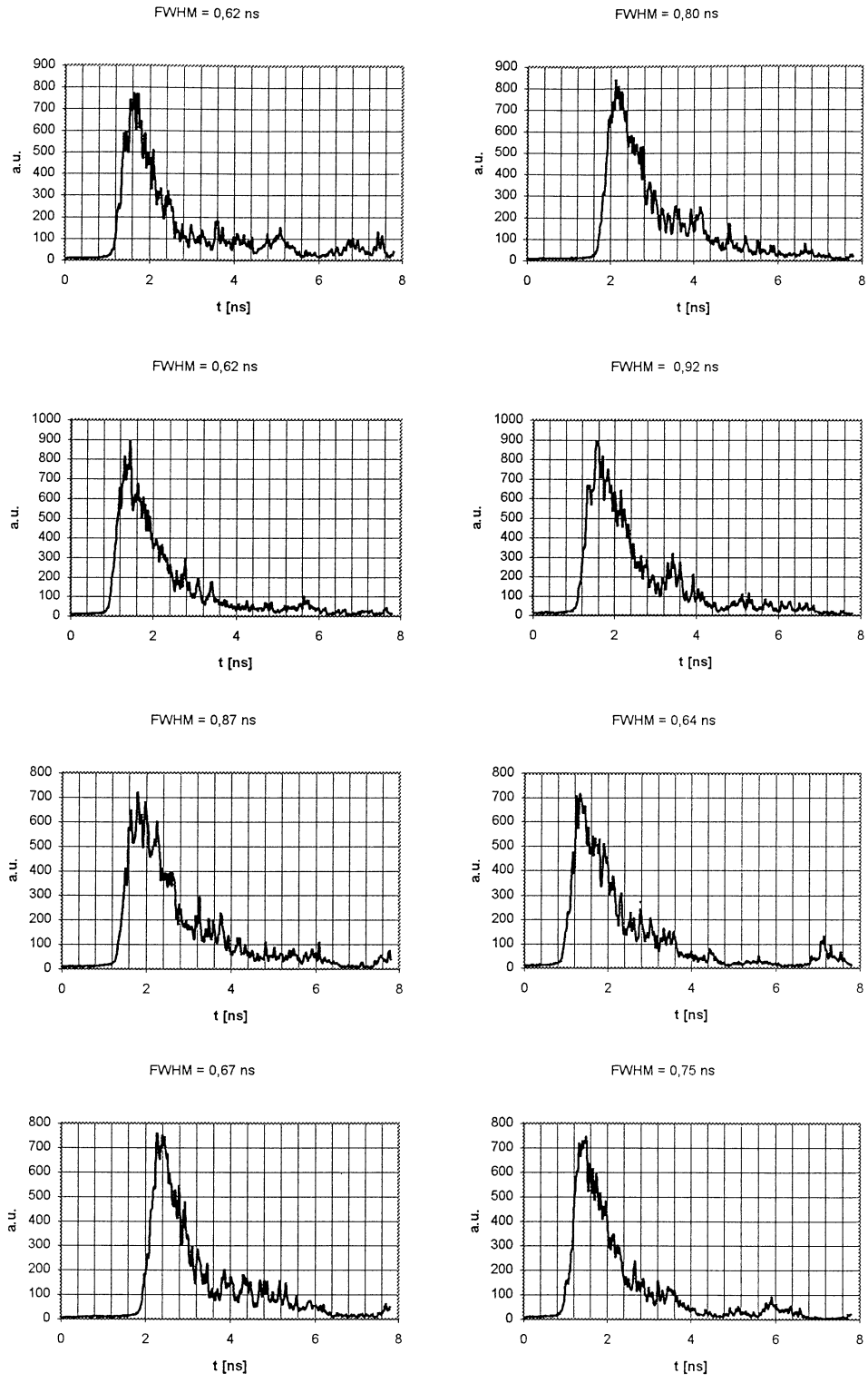

Figure 5-13 Pulse widths and shapes after the dye laser.

5.4.5 Doubling Crystal Output

The pulse was also measured after the KDP doubling crystal, placed after the dye laser (figure 5-14). The mean pulse width were 0.51 ns. In the figure, we can also see the best-obtained result so far, with a pulse duration of less than 300 ps.

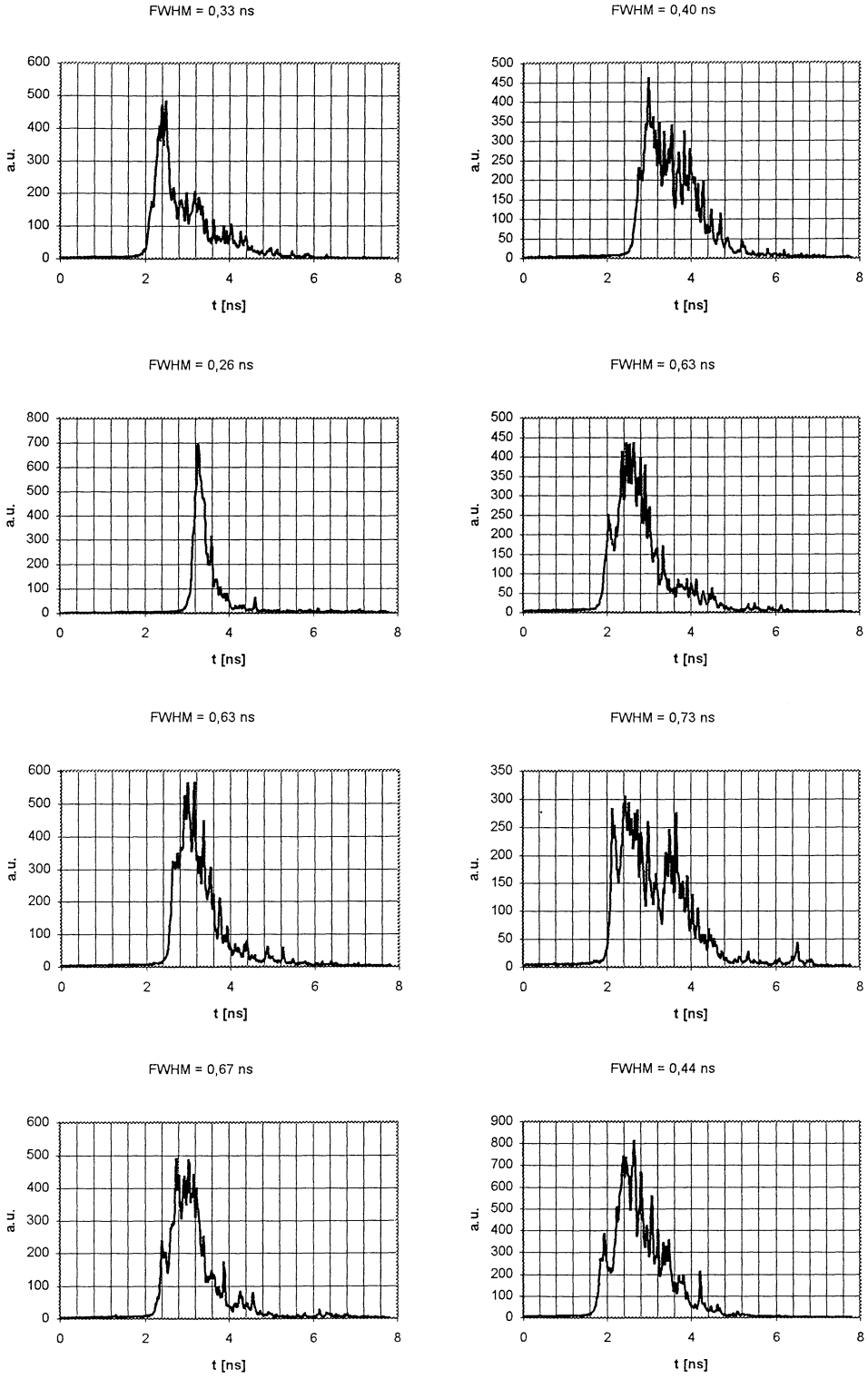

Figure 5-14 Pulse widths and shapes after the KDP frequency doubling crystal.

6 Conclusion

Stimulated Brillouin Scattering is a very promising method for producing sub-nano-second pulses. An SBS-compressor is easy to build and is, due to phase conjugation, very stable once inserted in the laser. Distilled water is suitable as active medium, since the Brillouin-gain is low enough to allow high pulse energies. The design with one amplifier and one oscillator cell works well, and by making the cells of glass, pollution of the water is avoided.

To obtain best results when using the compressor, the pulse energy must be high enough to initiate weak diffuse Brillouin scattering in the amplifier cell, without causing breakdown in the oscillator. By inserting a beam expander, this optimal energy can be varied. By fine tuning the performance, it is possible to get pulse widths below 1 ns after the dye laser.

So far, the beam has not been used for VUV-generation, but this will be tried in the near future.

7 Acknowledgements

First of all, I would like to thank my supervisor Claes-Göran Wahlström for making this interesting and challenging project possible.

I would also like to thank Li Zhongshan for his invaluable help with my work in the VUV laboratory, and for all the hours he has spent adjusting the dye laser.

Finally, I would like to thank Anders Persson for the help with the YAG laser and for knowing where to find all small things like mirrors, diodes, oscilloscopes, etc, and Sven-Göran Pettersson, for the help with the digital camera.

8 References

1. S. Svanberg, "Atomic and molecular spectroscopy", 2nd edition, Springer series on Atoms and Plasmas, 1992.
2. A. E. Siegman, "Lasers", University Science Books, 1986.
3. "Operation and Maintenance Manual NY80,81&82 Lasers", Continuum,1990.
4. R. W. Boyd, "Nonlinear Optics", Academic Press, 1992.
5. D. T. Hon, "Pulse compression by stimulated Brillouin scattering", Optics Letter **5** (1980), 516.
6. M. J. Damzen and M. H. R. Hutchinson, "High-efficiency laser-pulse compression by stimulated Brillouin scattering", Optics Letter **8** (1983), 313.
7. S. Schiemann, W. Ubachs and W. Hogervorst, "Efficient temporal compression of cohorent nanosecond pulses in a compact SBS generator-amplifier setup", IEEE Journal of quantum electronics **33** (1997), 358.
8. R. Y. Chiao, C. H. Townes, B. P. Stoicheff, "Stimulated Brillouin scattering and coherent generation of intense hypersonic waves", Physical review letters **12** (1964), 592.
9. C. B. Dane, W. A. Neuman, L. A. Hackel, "High-energy SBS pulse compression", IEEE Journal of quantum electronics **30** (1994), 1907.
10. I. L. Fabelinskii, "Molecular scattering of light", Plenum Press, 1968 (Original Russian text by Nauka Press, Moscow, 1965)
11. D. K. Cheng, "Field and wave electromagnetics", 2nd edition, Addison Wesley, 1989
12. L. D. Landau, E. M. Lifshitz, "Electrodynamics of continous media, volume 8 of course of theoretical physics", Pergamon press, 1960
13. R. A. Fisher, "Optical phase conjugation", Academic press, 1983
14. P. K. Kennedy, S. A. Boppart, D. X. Hammer, B. A. Rockwell, G. D. Noojin, W.P. Roach, "A first-order model for computation of laser-induced breakdown thresholds in ocular and aqueous media:partII-comparison to experiments", IEEE Journal of quantum electronics **31** (1995), 2250.
15. M. J. Damzen, M. H. R. Hutchinson, "Laser pulse compression by stimulated Brillouin scattering in tapered waveguides", IEEE Journal of quantum electronics **QE-19** (1983), 7.